USING GROUNDWATER MODELING TO UNDERSTAND THE FACTORS CONTROLLING LAKE SEEPAGE PATTERNS

A Thesis

Submitted to

The Temple University Graduate Board

in Partial Fulfillment

of the Requirements for the Degree

MASTER OF SCIENCE

By

James S. Mikochik

August, 2008

[redacted]

Dr. Laura E. Toran, Thesis Advisor

[redacted]

Dr. Jonathan E. Nyquist, Committee Member

[redacted]

Dr. George H. Myer, Committee Member

ABSTRACT

Understanding groundwater-lake interactions requires detailed knowledge of seepage patterns. Simple numerical models predict an exponential decrease of seepage with increasing distance offshore, but field measurements have shown that many lakes deviate from this pattern. To examine how hydrogeologic factors influence lake seepage patterns, two-dimensional steady state numerical models were constructed using the USGS modeling code MODFLOW. Sensitivity was tested to recharge, groundwater basin size and thickness, and lake morphology, as well as heterogeneities in lake sediment thickness and hydraulic conductivity, bedrock fracture zoning, and the effect of combining factors. The models were hypothetical, but many of the hydrogeologic parameters were based on those seen at Mirror Lake, a small glacial lake in New Hampshire. The models showed that increasing the thickness of lake bed sediments or decreasing their conductivity, increasing aquifer anisotropy, and decreasing the penetration of a lake into the groundwater system resulted in seepage rates that were more evenly distributed across a lakebed rather than focused near shore. Changing overall lake slope without increasing the penetration of the lake into the aquifer system produced little noticeable change in seepage patterns. Localized geologic heterogeneities, including a pinch-out in lake sediment and the presence of a high-K fracture zone, as well as a change in lake slope produced localized peaks in seepage. The peak produced by a pinch-out in lake sediment increased in magnitude as the degree of thinning increased, with seepage rates that locally were magnified by a factor of 150 where lake sediment was absent.

A high-K fracture zone produced a less significant peak whose size was controlled by several factors, including the overall length of the fracture, its connectivity to the lake, its orientation, and the presence or lack of low-K lake sediment. A change in lake slope produced a smaller peak compared with the pinch-out and fracture zone cases except when modeled using highly anisotropic conditions in which seepage rates were magnified by a factor of 20. Heterogeneities modeled closer to shore are more likely to contribute a significant amount of seepage to a water budget than those further from shore. One important factor controlling the degree of change in seepage was the contrast between lake bed sediments and the bedrock aquifer. Thus, the conductance of lake bed sediment and anisotropy should be measured to predict whether heterogeneities or breaks in lake slope will produce detectable localized changes in seepage rates. This modeling can help guide field studies by providing an understanding of the geologic conditions that control the rate of exponential decline of seepage away from shore.

ACKNOWLEDGEMENTS

This work was supported by the National Science Foundation Hydrologic Sciences Programs under Award No. 0609827. Without such help, none of this research would have been possible.

I would to thank Dr. Laura Toran for being an excellent thesis advisor. Not only did she provide me with a research opportunity, but she also provided countless advice, encouragement, and motivation through the beginning of my research up to the completion of my thesis. Her organizational skills and hard work ethic have been a great example for me. I would also like to thank my other committee members, Dr. Jon Nyquist and Dr. George Myer, who helped me transform and organize my research and ideas into a complete work ready to be read by the scientific community.

I would also like to thank all researchers studying groundwater-surface water interactions, especially Drs. Tom Winter and Don Rosenberry of the U.S. Geological Survey. My research and ideas would not exist had they not paved the way for me.

Not every master's student is blessed with being in such a great department as mine was. I would like to thank all of the Temple Geology staff, especially Shelah Cox and Drs. Terry, Grandstaff, Tumarkin-Deratzian, Ulmer, and Friel for providing me with an excellent educational experience. I would also like to thank fellow students including Natasha, Holly, Christian, Jesse, and Paul, as well as all other students, both graduate and undergraduate for not only being great companions along the way but also for providing me with great wisdom and encouragement.

Finally, I cannot forget the amount of help my parents, brothers, and friends have provided me throughout the years. Without them, I would not be the person who I am today.

TABLE OF CONTENTS

LIST OF TABLES

LIST OF FIGURES

CHAPTER 1
INTRODUCTION

1.1 Importance of Understanding Groundwater-Lake Interactions

Understanding the interaction between groundwater and lakes is crucial in assessing the problems associated with human as well as natural impacts on water quality and supply. Development along lakeshores has increased the likelihood of contaminant transport into lakes, for example, from septic systems (Guyonnet, 1991). Excessive withdrawal of water from local aquifers can cause unexpected reductions in the water levels of surface water bodies (Cherkauer and Nader, 1989), which are commonly used for recreational and commercial purposes. In addition, groundwater flux into lakes carries dissolved nutrients and buffers temperature, which are important for the survival of aquatic organisms (Rosenberry, 2005; Lee, 1977).

Surface water bodies, including lakes, are commonly discharge points for local groundwater flowsystems (Winter, 1976). Thus, the quality of lakes is dependant not only on the cleanliness of surface runoff but also on the quality of local groundwater. Although studies have focused on understanding the large-scale interaction between lakes and groundwater flowsystems (e.g. Winter, 1976), not enough attention has been focused on studying small-scale spatial variations in flow rates between groundwater and lakes at the sediment-water interface. This study examines such small-scale variations.

1.2 Seepage Studies in Lakes

Seepage is the flux per unit area (L/t or length/time) moving across the interface between a porous medium and open water or air (McBride and Pfannkuch, 1975). Out-seepage (usually expressed as negative values) refers to water leaving a surface water body and recharging the groundwater system; in-seepage (usually expressed as positive values) refers to water leaving the groundwater system and entering into a surface water body. Groundwater-surface water flux can be quantified using Darcy's Law:

$$Q = -KiA \tag{1}$$

Where Q is groundwater flux (L^3/t), K is the hydraulic conductivity of the porous medium (L/t), i is the groundwater gradient ($\Delta h/\Delta l$), and A is the cross-sectional area (L^2) perpendicular to the direction of groundwater flow.

While much time and resources have been devoted to understanding river-lake-atmosphere interactions and aquatic ecosystems, groundwater-surface water flux has generally been a misunderstood aspect of lake hydrological studies (Winter, 1976; Cherkauer and Zager, 1989). Water budgets performed on lakes typically measure only surface-water and atmospheric interchanges, assuming the contribution of groundwater to the budget to be the residual. This method is an inaccurate measure of seepage flux, considering the errors in measuring evapotranspiration and precipitation (Winter, 1976). In addition, the residual method does not provide information on amounts of in-seepage vs. out-seepage if the lake is flow-through (a lake that experiences both inseepage and outseepage) and also does not aid in identifying the spatial distribution of seepage across a lakebed (Winter, 1976, Asbury, 1990). Direct measurements of seepage in the field are thus a necessary component in creating an accurate water budget.

Most direct measurements of seepage have been conducted on small scales, covering only a portion of lake or stream. Such measurements have been performed using a variety of techniques, including temperature sensors, chemical tracers, electrical conductivity, piezometers, and seepage meters (Kalbus et al., 2006). Seepage meters (Figure 1-1), by far the most commonly used method of quantifying seepage, directly measure the flux of water across the sediment-water interface (Lee, 1977). The most common seepage meter setup consists of a 55 gallon drum cut in half, which is placed directly into lake sediment. A plastic bag filled with a known volume of water is tightly connected via tubing to an opening in the drum. Such a setup allows water to freely move into or out of the bag, and thus, a seepage rate for the area of lake encompassed by the drum can be calculated by measuring the change in the bag's water volume over a given time period.

Information from seepage studies has revealed that seepage can vary significantly both temporally and spatially. Temporal changes in the magnitude and direction of seepage have been reported in many studies that replicated seepage measurements within the same spatial location (e.g., Asbury, 1990; Sebestyen and Schneider, 2001; Woessner and Sullivan, 1984; Shaw and Prepas, 1990b). Seepage rates are also not distributed across the area of a lakebed evenly; they often spatially vary by orders of magnitude on large scales (tens to hundreds of meters) or small scales (meters or centimeters) (McBride and Pfannkuch, 1975; Kishel and Gerla, 2002). This spatial variability is thought to be influenced by the heterogeneity and anisotropy of local aquifers and lake sediments as well as complex lake morphology (Munter and Anderson, 1981). Cherkauer and McKereghan (1991) explored the affects of coastal morphology on seepage patterns along Green Bay and Lake Michigan. They observed that seepage rates were generally higher in embayment areas compared with coastal peninsulas. Small-scale variation, which is often neglected, can overwhelm larger-scale topographically driven seepage (Rosenberry, 2005), and can lead to false estimates of seepage patterns and water budgets if such factors are not taken fully into consideration.

Seepage meter studies, which are often performed in transects that are perpendicular to shore, have revealed that two distinct patterns exist in the spatial variability of seepage with relation to distance from shore. In some cases, an exponential decrease in seepage with increasing distance offshore exists. A study of seepage transects along Lake Williams, MN, revealed an exponential decrease in seepage (Erikson, 1981). Lee et al. (1980) observed a similar exponential decrease along three transects in Perch Lake, Ontario, although three other transects deviated from this pattern (Figure 1-2). A growing number of field studies have revealed that in most lakes, seepage rates decrease with increasing distance from shore by a weaker relationship. In such cases, either local minimum or maximum peaks in seepage or a shift in the slope of exponential decline occurs offshore (e.g., Rosenberry, 2000; Connor and Belanger, 1981; Anderson, 1987; Shaw and Prepas, 1990a,b; Kishel and Gerla, 2002; John and Lock, 1977). Some lake studies have even revealed a trend in which seepage rates increase away from shore (Woessner and Sullivan, 1984; Schneider et al., 2005).

Because seepage patterns have temporal and spatial variation, additional tools and techniques are needed to guide the placement of seepage meters. Geophysical techniques, for example, including electrical resistivity, seismic, and ground penetrating radar surveys, have been used to map subsurface heterogeneity patterns in order to identify potential zones of significant seepage (e.g. Taylor and Cherkauer, 1984; Anderson, 1987; Mitchell et al., 2008). Cherkauer and Nader (1988) used detailed geophysical measurements of low conductivity lake sediments on Green Bay, WI, in conjunction with seepage meter measurements and observed that seepage rates increased near regions of localized thinning in sediment thickness. Heaney (2007) used marine resistivity as a tool to identify shallow lake bed sediment heterogeneities in Lake Lacawac, PA. Although the groundwater contribution to the lake was small, the highest recorded rates using seepage meters were in the regions predicted by the geophysical signature of sediment pinch-out.

Another example of a useful tool to guide seepage studies is groundwater modeling. Groundwater models not only aid in calculating site-specific seepage flow rates, but are also useful in gaining a better understanding of the most important factors in influencing seepage patterns (Munter and Anderson, 1981; Krabbenhoft and Anderson, 1986).

1.3 Modeling Groundwater-Lake Interactions

Winter (1976) was perhaps the first to make use of groundwater models in understanding groundwater-surface water interactions within local and regional groundwater systems. His models were concerned with understanding the position, shape, and continuity of flow system divides beneath lakes. Thus, the factors influencing overall lake seepage volume and direction were analyzed. He concluded that the most influential factors were the height of the water table on the downslope side of the lake relative to lake level, the position of heterogeneities within the aquifer, and aquifer anisotropy (Winter 1976, 1981; Pfannkuch and Winter, 1984).

The distribution of seepage perpendicular from shore was another variable examined through groundwater models. McBride and Pfannkuch (1975) examined seepage using two-dimensional model of an inflow lake within a local groundwater basin (Figure 1-3). By plotting the log of seepage vs. distance from shore, they concluded that seepage decreases exponentially away from shore around a narrow band of the lake's perimeter under homogeneous conditions and when the width of the lake is small compared to the thickness of the aquifer. The presence of lake sediments of low hydraulic conductivity, which are common on lake bottoms, lowered the slope of exponential decline (McBride and Pfannkuch, 1975). Pfannkuch and Winter (1984) further examined factors that effect the distribution of seepage with distance from shore, and concluded that the following factors reduced the slope of exponential decline:

1) Small ratios of lake width/aquifer thickness
2) High values of anisotropy (K_x/K_y)
3) Deeper penetration of a lake bottom into the underlying aquifer

Models of both real and hypothetical lakes have been used to further understand factors that can lead to the exponential and non-exponential patterns that have been observed in seepage studies. Krabbenhoft and Anderson (1986) used a groundwater model to facilitate identification of the hydrological controls of an observed anomalous distribution of seepage along the Southeast shore of Trout Lake, Wisconsin. They concluded through modeling that a lens of coarse-grained material that intersected the lake bed could account for this anomaly (Krabbenhoft and Anderson, 1986). Cherkauer and Nader (1988) modeled localized thinning in lake sediment thickness, which produced an offshore peak in seepage near such a structure (Figure 1-4). Cherkauer and McKereghan (1991) explored models of different coastal configurations and concluded that the deeper an embayment penetrated into the local groundwater system, the more that groundwater flow converged around such a structure, resulting in a relative increase in seepage rates. Guyonnet (1991) modeled the effect of small-scale 50 cm thick heterogeneities on seepage patterns. He concluded that adding a continuous silt layer along a lake bottom spread seepage rates more uniformly through the lake. A discontinuous silt layer produced a high discharge peak to emerge offshore where the silt layer pinched out. He also observed that increasing the anisotropy ratio (the ratio of horizontal to vertical hydraulic conductivity, K_h/K_v) had a similar effect on seepage patterns as adding the continuous silt layer. Hypothetical lake models by Genereux and Bandopadhyay (2001) attempted to assess the sensitivity of additional lake and porous medium properties for both two-dimensional (2D) and three-dimensional (3D) settings. They observed that where a break in lake bed slope exists in a 2D setting, a significant non-exponential peak in seepage occurred when highly anisotropic conditions ($K_h/K_v \geq 100$) were applied (Figure 1-5). In the 3D models, they observed that the placement of highly conductive units that intersected the lake bed influenced the relative volumes of in-seepage vs. out-seepage that a flow-though lake experienced.

In summary, previous studies have shown that anisotropy, the thickness of the aquifer system below the lake or the degree of penetration of the lake into the aquifer system, and the overall thickness and hydraulic conductivity of lake sediments influence the slope of exponential seepage decline with increasing distance offshore. Studies have also shown that heterogeneities in the thickness and hydraulic conductivity of lake bed sediments, sediment lenses of a higher hydraulic conductivity than the surrounding porous medium, and changes in lake bed slope in highly anisotropic settings can create minimum or maximum peaks in seepage that deviate from the exponential decline of seepage away from shore.

1.4 Project Goals

Although some progress has been made in modeling the factors that influence seepage patterns, additional attention needs to be focused on assessing the sensitivity of known influential factors and also in investigating new potential factors. The goal of this project was to use the finite difference groundwater flow model MODFLOW to investigate the seepage patterns in a typical small glacial lake and local groundwater basin. The following factors were investigated:

1) The effect of lake sediment conductance, anisotropy, and aquifer thickness on varying the slope of exponential decline

2) The effect of localized geologic heterogeneities on seepage patterns, including variations in sediment thickness and K as well as fracture zones varied in length, position, distance from shore, and orientation

3) The effect of lake morphology on seepage patterns, including uniform slope variations and changes in lake slope

4) The effect of combining factors

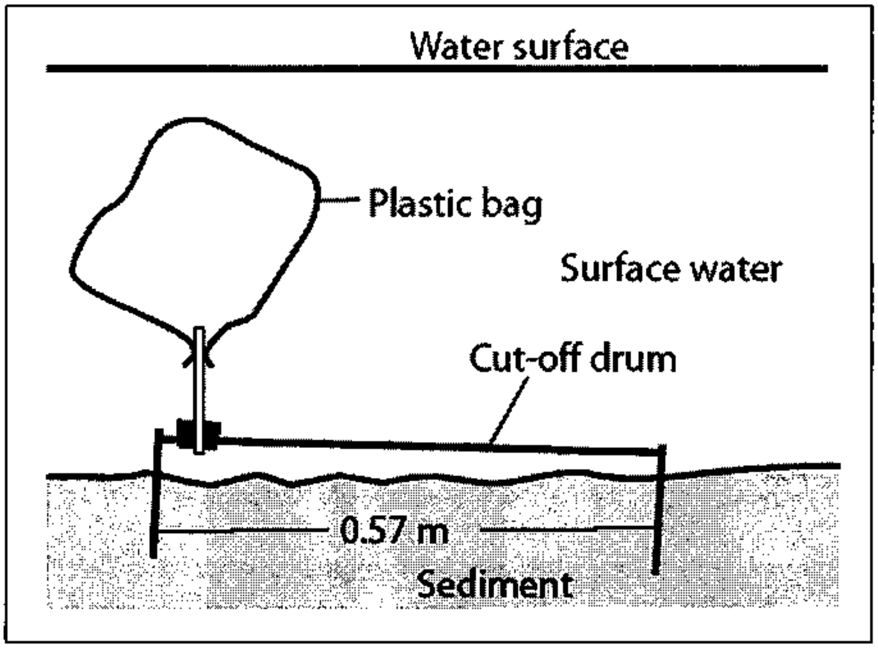

Figure 1-1: Original seepage meter design from Lee (1977).

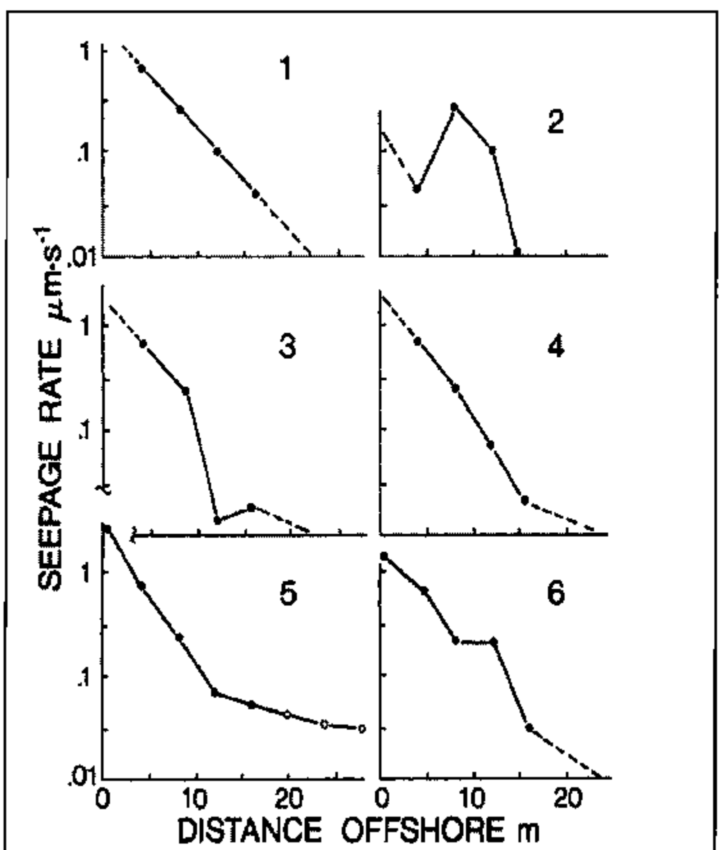

Figure 1-2:

Plots of seepage vs. distance from shore from several seepage meter transects along Perch Lake, Ontario (From Lee et al., 1980)

- Transects 1, 4, and 5 show an exponential decrease in seepage with distance from shore.

- Transects 2, 3, and 6, however, do not exponentially decrease away from shore.

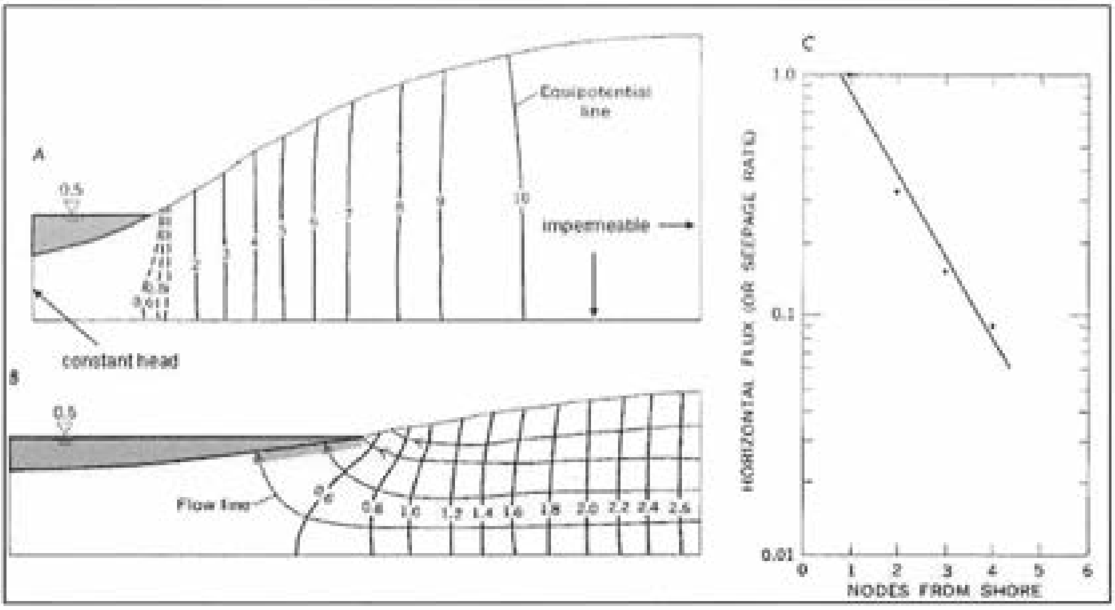

Figure 1-3:
2-D cross-sectional model of a hypothetical lake from McBride and Pfannkuch (1975).

A) Lake model showing head contours. The top boundary represents the water table.
B) Left third section of model showing how flow paths converge close to shore but spread out offshore.
C) Plot of seepage vs. distance from shore (expressed in nodes from shore).

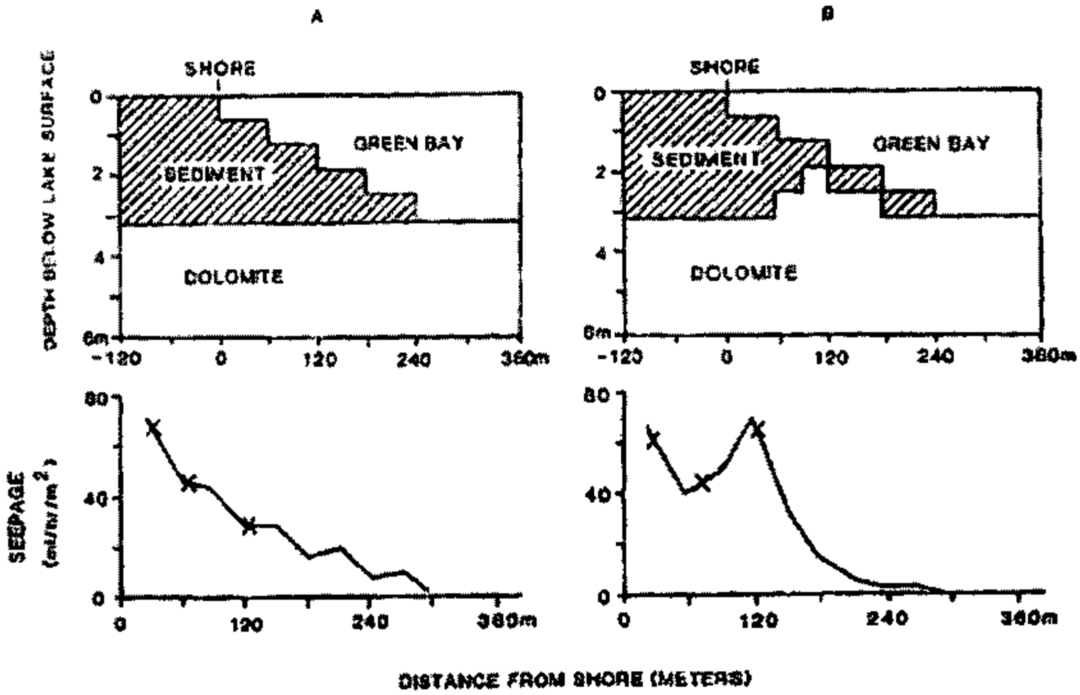

Figure 1-4:
Cross-sectional groundwater flow model of Green Bay, Wisconsin (From Cherkauer and Nader, 1988). The model shows sediment without (A) and with (B) localized thinning along with corresponding plots of seepage vs. distance from shore below each (field seepage data is included as the X's on the plots). Note that the localized thinning of sediment in (B) at 120 m from shore produces a sharp increase in seepage rates at that location.

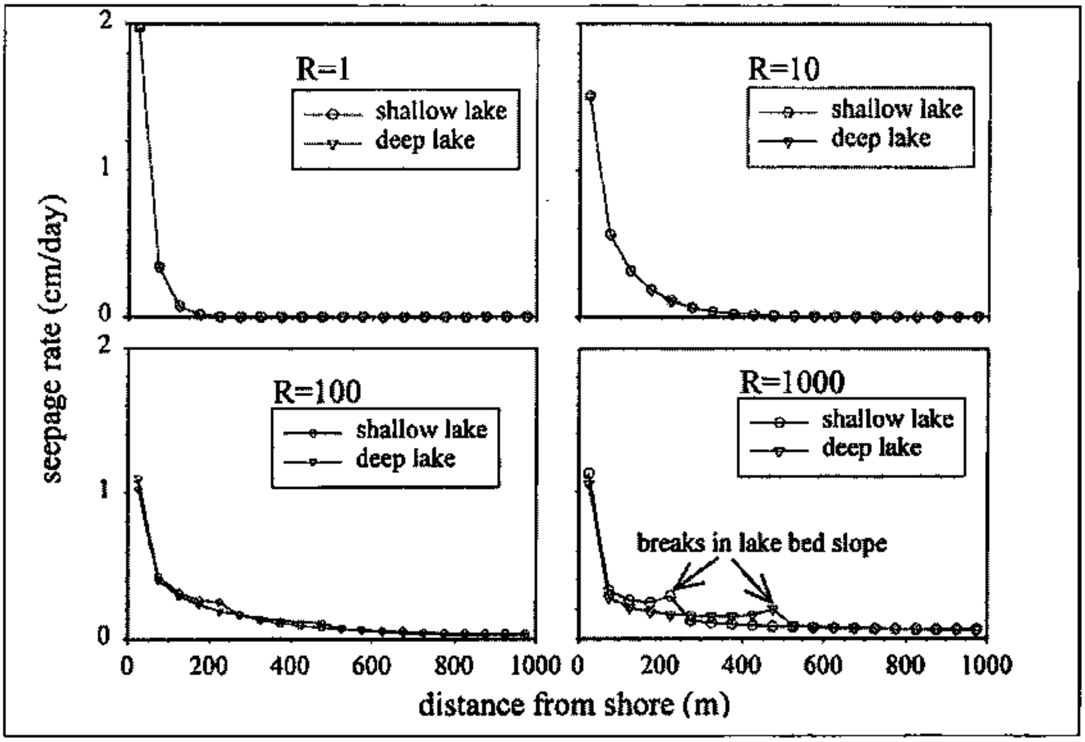

Figure 1-5:
Seepage transects from hypothetical lake models of various aquifer anisotropy ratios and lake depths from Genereux and Bandopadhyay (2001). Note that anisotropy is denoted as 'R' by the author (equivalent to K_h/K_v), not to be confused with recharge. The lake was constructed with a break in lake bed slope which was a greater distance offshore in the deep lake model than the shallow lake model. When K_h/K_v was modeled at values of 100 and 1000, slight peaks in seepage are noticeable at a distance corresponding to where these breaks exist.

CHAPTER 2
METHODS

2.1 Description of Software Used

The USGS "modular three-dimensional finite difference groundwater flow model" (McDonald and Harbaugh, 1988), or MODFLOW, was used to simulate groundwater-lake interactions in this study because of its wide variety of usage and application among groundwater hydrologists. Like other groundwater flow models, MODFLOW solves for head and flux within individual cells whose size and hydrologic properties are specified by the user. MODFLOW is a finite difference code, which represents the areas of interest using rectangular cells. Many previous studies have used MODFLOW to simulate groundwater-lake interactions (e.g. Tiedemann et al., 1998; Hunt et al., 2003; Genereux and Bandopadhyay, 2001)

Groundwater Vistas (GWV) version 4 (Environmental Simulations, Inc, 2004) was used as both a preprocessor and a postprocessor for MODFLOW. GWV allowed model boundary conditions and parameters for MODFLOW to be graphically input as well as the display of model results as head contours and flow rates.

2.2 Model Setup

The following section describes the generalized model setup used for all model runs, but not individual values input into MODFLOW, which are discussed in further detail in Sections 2.3 and 2.4.

A 2-D model was used in all model cases because of its simplicity in design as well as its success in producing useful results in previous hypothetical groundwater-lake studies (e.g., Winter, 1976; McBride and Pfannkuch, 1975; Guyonnet, 1991).

Although 3-D models can improve the accuracy and better represent the complexity of a site-specific groundwater-lake system, the goal of this study was to identify the most important parameters controlling seepage patterns, and thus, a simplified model was adequate for an initial study of patterns. Based on Genereux and Bandopadhyay's work (2001), the primary effect of 3-D modeling is to increase overall seepage rates (due to an increase in the recharge area). Steady-state conditions of groundwater flow were modeled since transient situations present further complexity in isolating the effect of parameters on seepage patterns.

The 2-D model was constructed as a profile (cross-section) configuration, which assumes that only flow in the x and z (depth) directions are occurring. Thus, in a lake-groundwater system, such a model is a vertical slice taken perpendicular to lake shore oriented parallel to the general direction of flow in the x-direction between the aquifer and lake. As described by Anderson and Woessner (1992) a profile model operates similarly to a one-layer 2-D aerial, except that the y-coordinate axis is treated as the z coordinate axis (Figure 2-1).

Because MODFLOW calculates certain aquifer parameters based on an x,y,z coordinate system, it is necessary to make some adjustments to ensure that such parameters are calculated appropriately. For example, the input recharge rate applied by the user for each cell is in the form L/t, which is then computed by MODFLOW over the area $\Delta x\ \Delta y$. However, in a profile model, recharge needs to artificially adjusted to occur along the top row cells over the area $\Delta x\ \Delta z$. The following formula was used to correct for this change (Anderson and Woessner, 1992):

$$R_m = R\ \Delta xz/\Delta xy = R\Delta z/\Delta y \qquad (2)$$

where R_m = recharge (L/t) required by profile model
R = recharge (L/t) applied to model (field value)

In all model cases, z (the model layer thickness) was set equal to a value of 1.0 m uniformly across the entire model. Thus, the correction process involved applying a recharge rate (R) that was a factor Δy higher than the required recharge rate (R_m). Recharge was applied at a constant rate to all aquifer (non-lake node) cells in the top model row.

A second adjustment needed in the profile model involved setting the aquifer as confined rather than as unconfined. Such an adjustment is necessary because in unconfined aquifers, the Boussinesq Equation is solved, and thus, the saturated thickness (h) is modeled with respect to the z direction. However, in a profile model, it is necessary to ensure that each cell is fully saturated, and thus, the saturated thickness is always equal to layer thickness (Anderson and Woessner, 1992).

The lake-groundwater system was simulated assuming a symmetrical basin in which all flow is diverted to a symmetrical inflow lake (a lake that experiences inseepage but not outseepage) (Figure 2-2). Thus, it is adequate to model only half of a lake, situating the center of the lake directly below a vertical no-flow boundary. The left, lower, and upper no-flow boundaries mark the extent of the groundwater flow system. Such a setup simplifies the interaction between lakes and groundwater so that only a single localized aquifer and the extent of the lake basin to which its flow is diverted are investigated. This setup, which has been established in many previous hypothetical groundwater-lake models (e.g., McBride and Pfannkuch, 1976;

Pfannkuch and Winter, 1984; Guyonnet, 1991) prevents the formation of multiple flow systems, allowing the main focus of the modeling to be the analysis of flux near the sediment-water interface between a single groundwater basin and lake.

Lake nodes were modeled using the General Head Boundary (GHB) package in MODFLOW. This head-dependant flow boundary type, which is often used to represent lakes and river of a fixed head that are underlain by sediment, calculates the flow between a specified head cell and aquifer cell as the product of the boundary cell conductance (C) and the difference between the boundary head (h_b) and the head of an adjacent aquifer cell (h) (Anderson and Woessner, 1992):

$$Q = C(h_b - h) \tag{3}$$

Thus, when $h_b > h$, flow occurs from the GHB cell to the aquifer, and when $h_b < h$, flow occurs from the aquifer to the GHB cell. The values for h_b and C are specified by the user, and C is defined as follows (McDonald and Harbaugh, 1988)

$$C = K_s A / b_s \tag{4}$$

where K_s = hydraulic conductivity of material between the GHB cell and aquifer
A = boundary area in the direction of flow
b_s = boundary thickness

When using GHB cells to model a lake of a specified stage (head), Q represents the flux between the groundwater system and the lake (Figure 2-3). Thus, seepage (L/t) can be calculated by dividing flux (Q) over a given area of lake bed (A). C represents the conductance of lake bottom sediments, which varies as a function of sediment thickness (b_s) and hydraulic conductivity (K_s). GHB cells were applied along a single one-cell-thick line of the model at the bottom of the lake.

2.3 Base Case Model Conditions/Parameters

All lake models used in this study were designed to represent the hydrologic and geologic conditions of small, glacially-formed kettle lakes. Many of these conditions were based on of data collected by Winter (1984), Tiedeman et al. (1998), and Mitchell et al. (2008) from Mirror Lake, NH. However, the models were not designed to recreate this exact groundwater-lake system, nor were the conditions used in the models limited to data collected from this particular location. Data and insight from additional site-specific or hypothetical kettle lake studies, including Guyonnet (1991), Genereux and Bandopadhyay (2001), and Munter and Anderson (1981) were also used as justification for the model parameter values used.

Because varying model conditions/parameters to view their effect on changing lake seepage patterns was the focus of this study, it was necessary to establish a base-case model with set boundaries and parameter values for comparison. These boundary conditions and values mentioned in this section were used for model runs except where variations are specified in Section 2.4. In all cases, including the base case, dimension and time values applied to the model are expressed in terms of meters and days, respectively.

The base case was divided into 43 rows and 610 columns of variable cell size, producing a model domain that was 1250 m long (x), 42 m wide (y), and 1 m thick (z). However, since a profile model configuration was used (see Section 2.2), MODFLOW x, y, and z directions represent groundwater basin length, thickness, and width, respectively. The ratio of basin length (from edge of basin to center of lake) to aquifer thickness (~30:1) was modeled after ratios used from previous hypothetical lake studies such as Guyonnet (1991), who used a ratio of 25:1 and Genereux and Bandopadhyay (2001), who used a ratio of 60:1. The thickness (y dimension) of the cells varied between 0.5 m in the top 30 rows, gradually increasing in rows 31 - 43 to a maximum of 4.5 m. The length of the cells (x dimension) varied gradually from a maximum of 10 m transitioning to 0.5 m in columns 1 – 110 and was held uniform at 0.5 m from columns 111 – 610. Thus, the region encompassed by rows 1 – 30 and columns 110 – 610 were refined to cells sized 0.5 m x 0.5 m to allow the placement of small-scale heterogeneities below the lake. The region of cell refinement, therefore, encompasses half of a lake 250 m in length and 10 m deep at maximum, which approximates the dimensions of Mirror Lake (Winter, 1984). The lake was simulated using 500 GHB cells representing the lake bottom placed to simulate the common break in slope morphology of a lake bottom, slanted along the shore and flatter in the middle (Figure 2-4). The boundary head of each cell (lake stage) was set uniformly at 50 m, and the conductance term for each cell was set uniformly at 1 m^2/day with K_s = 1 m/day and b_s = 0.5 m.

The hydraulic conductivity of porous medium cells (K_a) was modeled using a homogeneous and isotropic value of 1 m/day, typical of medium to fine sand (e.g. Freeze and Cherry, 1979). Thus, since GHB conductance was set at 1 m^2/day and each porous medium cell in proximity to the lake was 0.5 m thick with K_a = 1 m/day (and thus, also a conductance 1 m^2/day), there was no contrast in hydraulic properties between the porous medium and lake sediment in the base case model setup.

A recharge rate of 1.13×10^{-3} m/d was used, which was calculated based on an average annual precipitation rate for New Hampshire of 124 cm/year, as recorded between 1978 to 1986 by Federer et al. (1990). It was assumed that on average recharge to an aquifer is 1/3 the precipitation rate in humid climates. Because the width (Δy) of each cell in the first row is 0.5, the actual recharge rate required by the profile model setup (R_m), as calculated by Equation 2, was 2.27 x 10^{-3} m/d.

2.4 Model Parameter Variations

Model parameter conditions of the base case model described in Section 2.3 were varied (Table 2-1) to determine the effects on seepage patterns. The following section describes the parameters/conditions that were varied in model runs as well as the range of values used.

Parameters that were varied individually (termed "single-variable parameters") included variable recharge (R), groundwater basin length (L), aquifer thickness (b_a), lake slope (θ), the degree of break in lake slope (Φ), anisotropy (K_x/K_y), the conductance (C) of lake bed sediments on both a regional and localized scale, and the positioning of high-K fracture zones (Figure 2-5). Other model runs combined the effect of more than one individual parameter, termed "multiple variable parameters."

2.4.1 Single Variable Parameters

2.4.1.1 Recharge

Recharge (R) was changed by altering the base recharge rate (1.13 x 10^{-3} m/d, or 1/3 of precipitation) to recharge rates 2/3 (2.27 x 10^{-3} m/d), 1/6 (5.57 x 10^{-4} m/d), 1/12 (2.83 x 10^{-4} m/d), and 1/24 (1.42 x 10^{-4} m/d) of precipitation. Because recharge cannot exceed precipitation, recharge rates higher than 2/3 of precipitation were not modeled.

2.4.1.2 Groundwater Basin Size

Groundwater basin size was varied by adding or subtracting model columns, thus, increasing/reducing the size of the model grid x-direction. The lake radius was held constant at 250 m, and variations are expressed in terms of the ratio of basin length (L) to lake radius (r). Six variations were modeled, using L/r = 1, 2, 3, 4, 5, and 7.

2.4.1.3 Aquifer Thickness

Aquifer thickness was varied by adding/subtracting cells to or from the bottom rows, thus, increasing/reducing the size of the model grid y-direction. The maximum lake depth was held constant at 10 m, and variations are expressed in terms of aquifer thickness (b_a) to maximum lake depth (d). Twenty-one values of b_a/d were modeled, ranging from 1.5 to 50.

2.4.1.4 Lake Sediment Conductance

Lake sediment conductance (C) was varied uniformly by altering the hydraulic conductivity and thickness inputs in the GHB package. A conductance of 1 m^2/d was set as the base case model run because this rate represents a conductance equivalent to that of the surrounding porous medium cells. Modeled conductance rates, although expressed in m^2/d, can be imagined to represent any combination of sediment thickness (b_s) and hydraulic conductivity (K_s), given that GHB cell thickness and width are held constant (see Equation 4). If 0.5 m thick sediment is assumed, the model value of C (m^2/d) is equal to K_s. Rates were varied over a range of conductance values (17 total between 1 m^2/d and $1e^{-5}$ m^2/d), thus, accounting for a large range of contrast between aquifer and sediment conductivity. Values higher than

1.0 m^2/d were not modeled under the assumption that lake sediments are usually of a lower conductivity than aquifer material. Such a range of contrast in hydraulic properties (a factor of 10^5) exists in glacial-lacustrine sediments in Mirror Lake, which range from 2.9 x 10^{-4} m/s within glacial outwash to nearly 10^{-10} m/s within lacustrine mud (Tiedeman et al., 1998).

Localized heterogeneities within lake bed sediment were modeled by modifying GHB conductance rates within a 5 m zone at a location between 20 m to 25 m from shore. The distance that variations in seepage have been observed varies from near shore to distances of 10's of meters. The surrounding sediment along most of the lakebed was assigned a conductance of 0.0025 m^2/d (the equivalent of 0.5 m-thick sediment with K_s = 0.01 m/d), which was gradually adjusted by increments of increasing conductance towards the center of the heterogeneity location (approximately 22.5 m offshore). If a uniform K_s of 0.01 m/d is imagined to apply to all GHB cells in the lake model, the localized heterogeneity can be perceived as a pinch-out in sediment thickness at the heterogeneity location (Figure 2-6). For example, a pinching-out from 200 cm to 50 cm thick sediment was modeled by gradually changing 0.01 m/d sediment from a thickness of 200 cm (C = 0.0025 m^2/d) to 50 cm (C = 0.01 m^2/d), thus, creating a 4x contrast in conductance. Each of the pinch-out variations are named based on the percent of sediment pinch-out at the heterogeneity location. Thus, the above example would be a 75% pinch-out. Six variations in sediment pinch out were modeled, including 0% (no pinch-out), 50%, 75%, 95%, 99.5%, and 100% (full pinch-out). Likewise, the localized heterogeneity can also be imagined as a change in K_s that occurs over sediment of a constant thickness (Figure 2-6). If the sediment is assumed to be 0.5 m thick across the entire lake bottom, K_s is equal in value to the conductance term assigned to any given cell.

In addition to varying pinch-out percent, the distance from shore at which this heterogeneity was placed was varied to understand how spatially varying its position from shore effected seepage patterns. The pinch-out was placed at distances of 2.75 m, 12.75 m, 22.75 m, 32.75 m, 42.75 m, 52.75 m, and 62.75 m from shore.

A gradual change offshore in K_s or b_s, which represents a more regional rather than localized sediment heterogeneity, was modeled by changing the conductance settings applied to each GHB node with respect to distance from shore. Such a parameter was modeled by decreasing GHB conductance rates from 0.5 m^2/d (1^{st} node from shore) to 0.005 m^2/d (200^{th} node from shore) along 100 m, which was achieved using two different approaches: K_s was decreased linearly by 0.002 m/d per cell in the first variation and b_s was increased linearly by 0.5 cm per cell in the second variation (Figure 2-7).

2.4.1.5 Fracture Zone

Fracture zones were created in the lake models to represent single thin, localized heterogeneities not associated with lake bed sediment that could be varied in length (F_L), connectivity to lake (F_c), and orientation (F_ψ) (Figure 2-8) to better understand the effects of such variations in controlling seepage patterns. All fracture zones were modeled with a thickness of 0.5 m and were assigned a hydraulic conductivity of 100 m/d (100x more conductive than surrounding cells). Fracture zone length was modeled by varying a single, vertical fracture zone in place at a distance 22.75 m from shore. Variations in this parameter included 0 m (no fracture zone), 4 m, 8 m, 12 m, and 24.5 m. Fracture zone connectivity to the lake cells was varied by increasing the cut-off distance between the termination of the cells assigned as fracture zones and the lake cells. A long fracture (35.5 m to 39.5 m) was used for the connectivity variations. Thus, the length "cut-off" from the fracture zone was minimal compared to the entire length of the fracture zone itself. The distance from shore at which a vertical fracture zone was placed was varied to understand how spatially varying its position from shore effected seepage patterns. The fracture zone was placed at 2.75 m, 12.75 m, 22.75 m, 32.75 m, 42.75 m, 52.75 m, and 62.75 m from shore. Finally, fracture zone orientation was varied by changing the angle F_{ψ} that the zone was placed with respect to horizontal (model x-direction). Angles of 45°, 90°, 116.6°, 135°, 153.4°, and 180° were modeled, which were limited by the finite-difference grid design.

2.4.1.6 Anisotropy

Anisotropy was modeled by varying the ratio of horizontal hydraulic conductivity (K_x) to vertical hydraulic conductivity (K_y) within porous medium cells. Nine values of K_x/K_y were modeled: 1, 2, 5, 10, 20, 50, 100, 200, and 500. Values of K_x/K_y larger than 100 are not uncommon in field settings (Winter, 1976) and are sometimes even necessary to calibrate groundwater models with observed field data (e.g., Munter and Anderson, 1981).

2.4.1.7 Lake Morphology (Slope)

Lake slope (θ), expressed in degrees with respect to horizontal (model x-direction), was varied by uniformly increasing or decreasing the number of lake cells per row while maintaining a maximum lake depth of 10 m. Thus, the actual slope angles modeled were limited by the finite-difference grid setup. Five angles were modeled: 2.9°, 3.8°, 5.7°, 8.1°, and 11.3° (Figure 2-9). Angles higher than 11.3° are not included within this set of variations due to the interference in seepage patterns created by a break in slope offshore. Offshore breaks in lake slope from a steeper lake bed angle transitioning at an offshore vertex point to a flat (0°) lake bed were modeled using various vertex angles (Φ), expressed in degrees, including Φ = 8.1°, 11.3°, 18.5°, and 26.6°. A lake bottom that experiences multiple breaks in slope (including an upper and lower break in slope of an equal vertex angle of 26.5°) was also modeled. Bathymetry surveys of Mirror Lake using GPR methods indicated that upper breaks in slope as high as Φ = 27° and lower breaks in slope as high as Φ = 22° exist along the lake bottom (Mitchell et al., 2008).

2.4.2 Multiple Variable Parameters

The following parameters were combined (see Table 2-1 for more specific details):

1) A high-K fracture zone (of consistent length, connectivity to lake, and hydraulic conductivity) combined with sediment of variable conductance, combined with various aquifer anisotropy, and combined with various aquifer thickness

2) A change in lake slope (Φ = 26.6°) due to lake sediment pinch-out (Figure 2-10)

3) A change in lake slope (Φ = 26.6°) combined with sediment of variable conductance, combined with various aquifer anisotropy, and combined with various aquifer thicknesses

4) Multiple breaks in lake slope

Although more combinations are possible, those listed above were chosen in order to better understand how the interaction between large scale geologic parameters (such as the conductance of sediments across the entire lake bed, overall aquifer thickness, and overall aquifer anisotropy) and small-scale geologic parameters (such as localized sediment thinning and fracture zones) influence seepage patterns.

2.5 Data Processing

Because the distribution of seepage relative to distance from shore was the focus of this study, the flux values calculated by MODFLOW between GHB cells and adjacent aquifer cells were the primary values used in comparing the results of different model runs. However, in a few cases, the distribution of model calculated head values in cells below the lake nodes served as a useful illustration of the effect of parameter variations in controlling lake-groundwater interactions.

To process flux data more quickly and efficiently, the Groundwater Vistas boundary reach feature was used. Normally, this feature is used to assign reaches to different portions of a river or stream that is modeled using head-dependant boundary cells, but it proved to be useful in assigning each GHB lake node a particular reach number based on its distance from shore. Each GHB cell was assigned a particular reach number starting with 1 for the cell closest to shore and increasing by increments of 1 each cell offshore (Figure 2-11). The boundary reach report command in Groundwater Vistas was then used to export the data as a comma-separated variable (.csv) file with each reach number along with the model calculated flux along each reach in L^3/t (m^3/day). The flux values for each reach were then divided by the cell area in the x,z model direction (0.5 m^2) and converted to cm/day, the unit of measurement most commonly used in lake seepage studies. Assuming that this measurement represents the seepage rate at the midpoint of each lake cell and that the shoreline represents the start of the seepage transect (0 m), seepage (cm/day) can be expressed as a function of distance from shore on a semi-log plot.

The use of a finite-difference grid model presented a slight obstacle in modeling seepage patterns due to an artifact caused by having multiple GHB cells in each row. Such a configuration, rather than producing an evenly-sloped lake bottom, produces a "stair-step" structure since some of the lake cells (the 1st GHB cell in each row) share a horizontal as well as a vertical face with the porous medium cells. This 'stair-step' morphology due to the finite-difference grid resulted in an oscillating seepage pattern with an upward peak near the first row cell decreasing to a downward peak towards the end row cell. The peaks repeated at the start of each row by the same factor, producing the oscillation pattern (Figure 2-12). Such a pattern was also observed by Genereux and Bandopadhyay, 2001, who used MODFLOW as well as a grid design similar to that used in this study consisting of multiple lake node cells per row. The pattern dissipates after the offshore break in slope where the lake is horizontal and GHB cells only share one face of porous medium.

Although this artifact produced a slight challenge in correctly interpreting the model data, the overall trend reveals that seepage still decreases from shore at an exponential rate (Figure 2-12). Furthermore, the relative change produced by this oscillation repeats by the same amount at a given cell number in each row. Plotting a single cell in each row shows the decline without oscillation; thus, a consistent cell in each row is used in data analysis for each model variation. For most of the modeling results, the 6th cell in each row was used, since it approximately represents the average seepage rate for a given row. When lake bed slope variations were the parameter analyzed, the 1st cell in each row was used because this cell always lies at the point where a break in slope exists.

If the model parameter produced an exponentially decreasing seepage patterns that changed in slope or shifted the exponential pattern upward/downward, an exponential fit trend for each parameter value's data was performed using the following general formula (modified after Shaw and Prepas, 1990a):

$$\text{Seepage (cm/day)} = \alpha e^{-\beta x} \qquad (5)$$

where α = y intercept
β = value of exponent (or the slope of the line on a semi-log plot)
x = distance from shore (m)

Plots of β and α as a function of the modeled parameter values were useful for comparing the sensitivity of various parameters in controlling the degree of exponential decline. In addition, the coefficient of determination (R^2) was calculated for such parameters. If R^2 for any model run was below 0.95, the departure from linearity is discussed in further detail.

If the model parameter produced local minimum or maximum peaks that deviated from the exponential decrease in seepage from shore, the magnitude change in the peak (M) was calculated for each model run by dividing the peak value by an estimate of the seepage rate at that distance without the peak. This estimate was performed by fitting an exponential function to points further offshore from the peak value that exhibited a clearer exponential trend. This approach yielded a good estimate of the magnitude of change in seepage produced by each parameter value.

2.6 Summary

Two-dimensional, steady-state profile models of hypothetical lakes were created using MODFLOW and using Groundwater Vistas version 4 as a pre and post-processor. The lakes were designed to represent the hydrogeologic conditions seen in small, glacially-formed kettle lakes. Many of these conditions were based off of Mirror Lake, NH and its local groundwater basin as well as other conditions used in previous studies that modeled hypothetical or site-specific lakes. Specific model parameters were varied both individually and together to understand how they influence lake seepage patterns. Seepage rates from each model run were plotted as a function of distance from shore on a semi-log scale. Parameters that influenced the degree of exponential decline of seepage from shore were fit to exponential functions, and parameters that produced deviations from this exponential trend were analyzed to assess the degree of deviation they produced.

Table 2-1:

Full list of parameter variations. Included are variable names, symbols used, and range of values modeled.

Parameter/Feature	Range of Values Modeled
Recharge (R)	R = 1/24, 1/12, 1/6, 1/3, and 2/3 of precipitation
Ratio of basin length (L) to lake radius (r)	L/r = 1, 2, 3, 4, 5, 7
Ratio of aquifter thickness (b_a) to max. lake depth (d)	b_a/d = 1.5, 1.75, 1.85, 2, 2.25, 2.5, 2.75, 3, 3.5, 4, 4.2, 5, 6, 7.5, 10, 12.5, 15, 20, 25, 35, 50
Uniform GHB sediment conductance	C (m^2/d) = 0.00001, 0.0001, 0.001, 0.00125, 0.0025, 0.005, 0.01, 0.02, 0.025, 0.04, 0.05, 0.08, 0.1, 0.16, 0.32, 0.64, 1.0,
Localized sediment thinning (pinch-out)	Percent thinning of sediment: 0%, 50%, 75%, 95%, 99.5%, 100%
Pinch-out distance from shore	Distance from shore (m) = 2.75, 12.75, 22.75, 32.75, 42.75, 52.75, 62.75
Gradual change offshore in K_s or b_s	Change in C of 0.5 m^2/d to 0.005 m^2/d along a 100 m transect by (1) linearly decreasing K_s by 0.0025 m/d per cell and (2) linearly increasing b_s by 0.5 cm per cell
Fracture zone length (F_L)	F_L (m) = 4, 8, 12, 24.5
Fracture zone connectivity to lake (F_c)	F_c (m) = 0.5, 1.0, 2.0, 4.0
Fracture zone distance from shore	Distance from shore (m) = 2.75, 12.75, 22.75, 32.75, 42.75, 52.75, 62.75
Fracture zone orientation (F_ψ)	F_ψ = 45°, 90° (Vertical), 116.6°, 153.4°, 135°, 180°
Anisotropy Ratio (K_x/K_y)	K_x/K_y = 1, 2, 5, 10, 20, 50, 100, 200, 500
Uniform Lake Slope (θ)	θ = 2.9°, 3.8°, 5.7°, 8.1°, 11.3°
Break in lake slope or vertex angle (Φ)	Φ = 8.1°, 11.3°, 18.5°, 26.6°
Multiple breaks in lake slope	Φ_1 = -26.6°, Φ_2 = 26.6° (upper and lower breaks in slope, respectively)
High-K fracture zone with variable GHB C	C (m^2/d) = 1.0, 0.5, 0.2, 0.1, 0.05, 0.02, 0.01
Break in lake slope (Φ = 26.6°) combined with variable GHB C	C (m^2/d) = 1.0, 0.5, 0.2, 0.1, 0.05, 0.02
Fracture zone combined with anisotropy	K_x/K_y = 1, 10, 100
Break in lake slope (Φ = 26.6°) combined with anisotropy (K_x/K_y)	K_x/K_y = 1, 2, 5, 10, 20, 50, 100, 200, 500
Break in lake slope (Φ = 26.6°) with lake sediment pinch-out	Break in lake slope modeled with and without sediment pinch-out, compared to a pinch-out without a break in lake slope

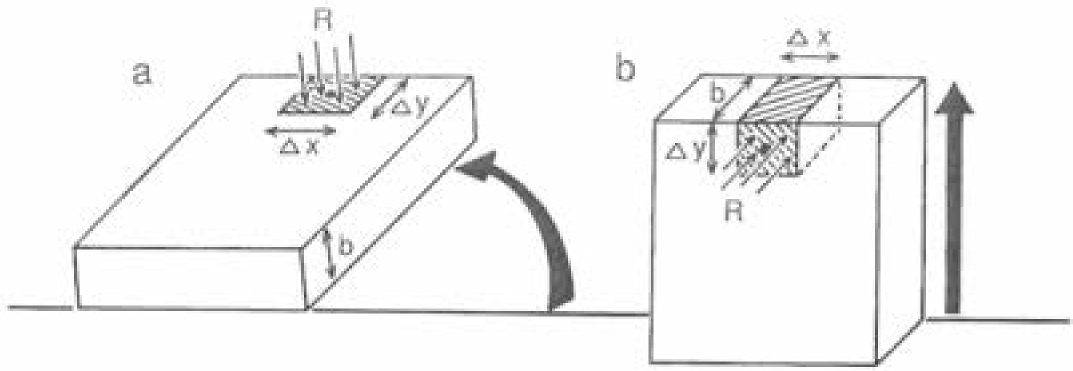

Figure 2-1:

Illustration of a profile model setup.
(a) Standard areal 2-D model with recharge applied over the area Δx Δy.
(b) Orientation required for profile model setup. Recharge is still applied to the area ΔxΔy, but must be adjusted manually to occur over the area Δx Δz(b) if Δy and Δz are of a different value. From Anderson and Woessner (1992).

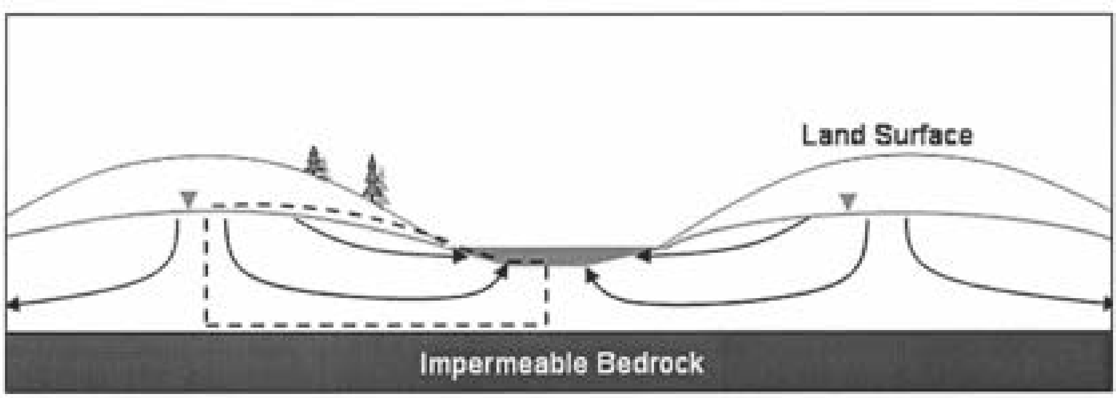

Figure 2-2:

Illustration of the interaction between a symmetric groundwater basin whose flux is diverted to an inflow lake. The extent of the model non-flow boundaries for this particular study, shown in dashed lines, encompasses a region of localized recharge that flows entirely into a zone of localized discharge (lake).

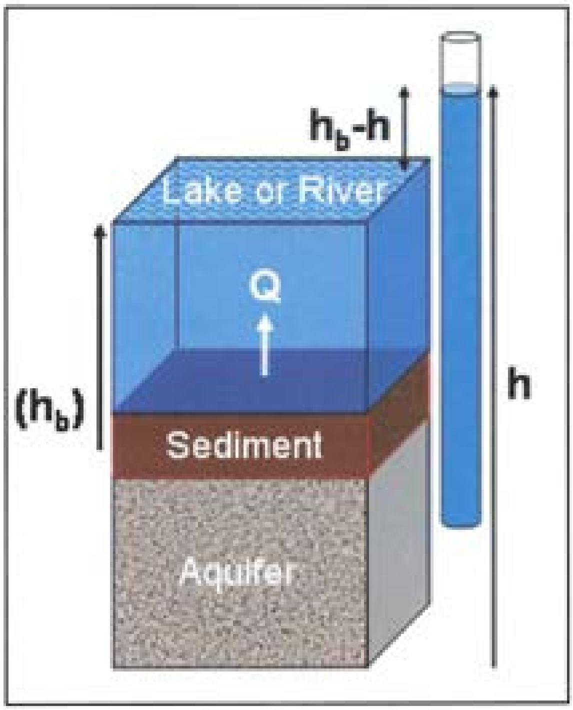

Figure 2-3:

Representation of a MODFLOW general head boundary. The flux (Q) between a body of water of specified head (h_b) and aquifer head (h) is calculated as the product of h_b-h and the conductance of sediments between the body of water and aquifer.

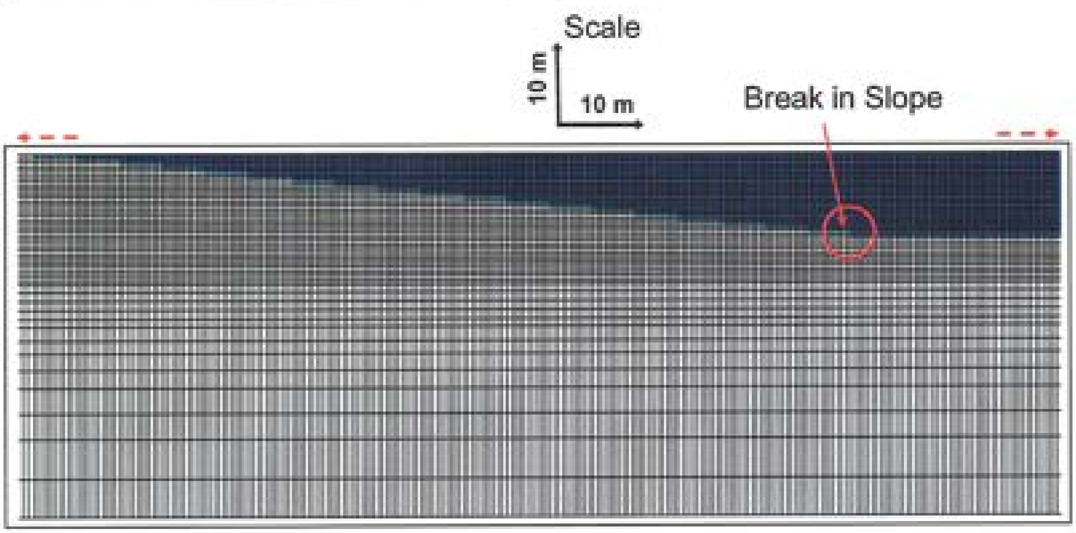

Figure 2-4:
View of the base case grid setup and boundary conditions in Groundwater Vistas. Note that this is only a partial view of the grid, as indicated by the red arrows. Dark blue cells are no-flow cells, light blue are GHB cells, and white are porous medium cells. The GHB cells were placed in such a fashion to resemble the common break in slope morphology of a lake bottom, slanted along the shore and flatter in the middle.

A)

B)

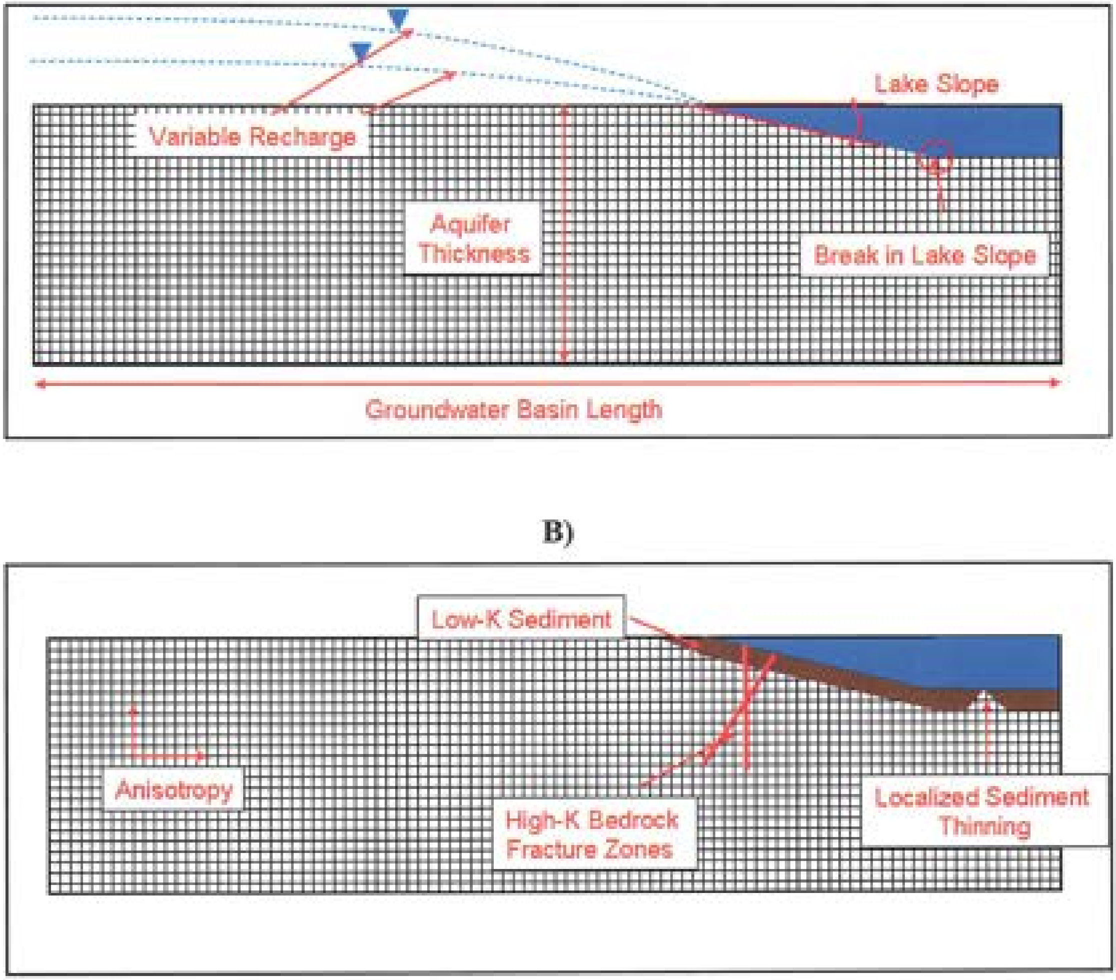

Figure 2-5:

Illustrations showing the varied hydrogeologic parameters in this study.
A) recharge, aquifer thickness, basin length, lake slope, and break in lake slope.
B) anisotropy, sediment K and thickness, and high-K bedrock fracture zones.

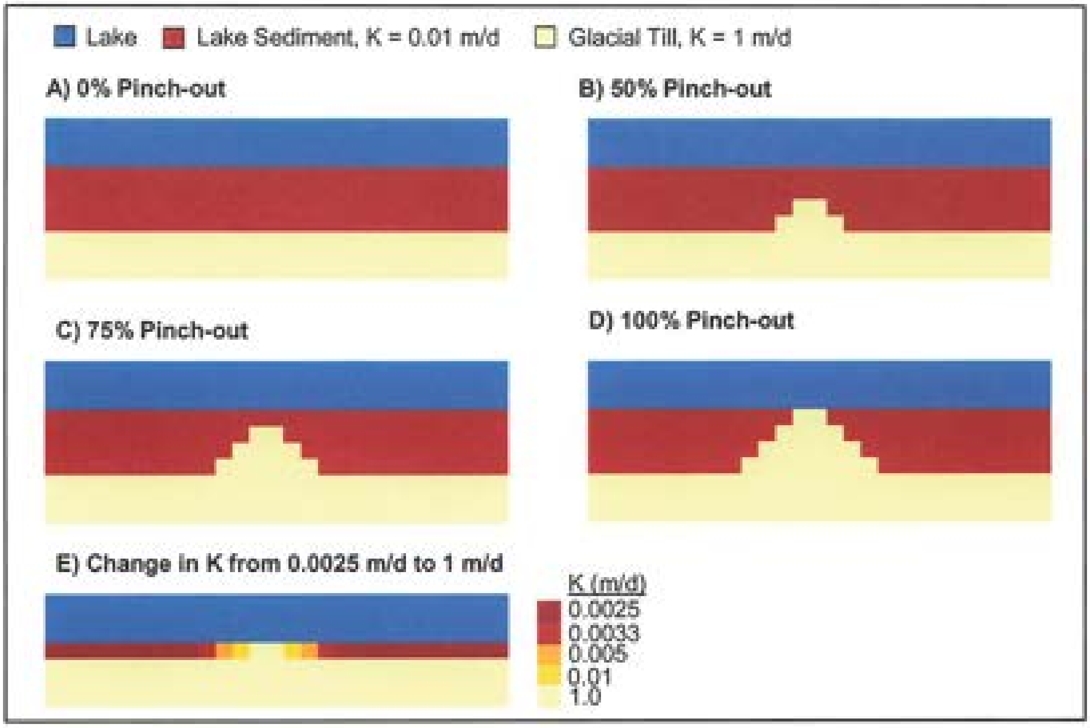

Figure 2-6:
Illustration of four of the six modeled pinch-out thicknesses assuming a uniform lake sediment K of 0.01 m/d. Thus, the "pinching out" represents sediment thickness at the zone of greatest localized thinning (22.5 meters from shore). The localized heterogeneity can also be perceived as a change in K, assuming a constant thickness. 'E' is analogous to 'D', assuming a uniform sediment thickness of 0.5 m

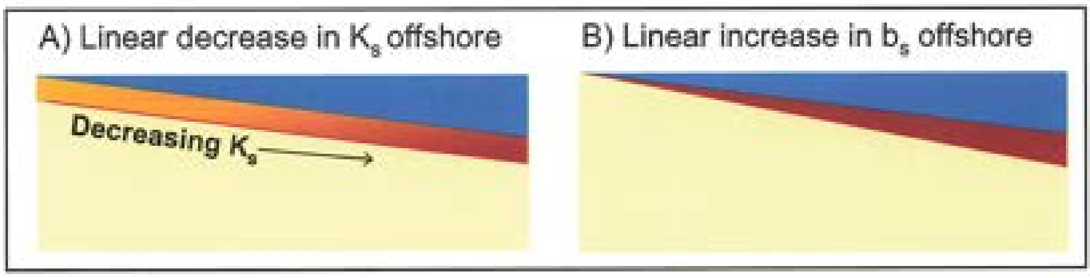

Figure 2-7:
Illustration of a gradual change in conductance of 0.5 m^2/d to 0.005 m^2/d offshore. This was achieved by A) linearly decreasing K_s offshore using a fixed value of b_s and B) linearly increasing b_s offshore using a fixed value of K_s.

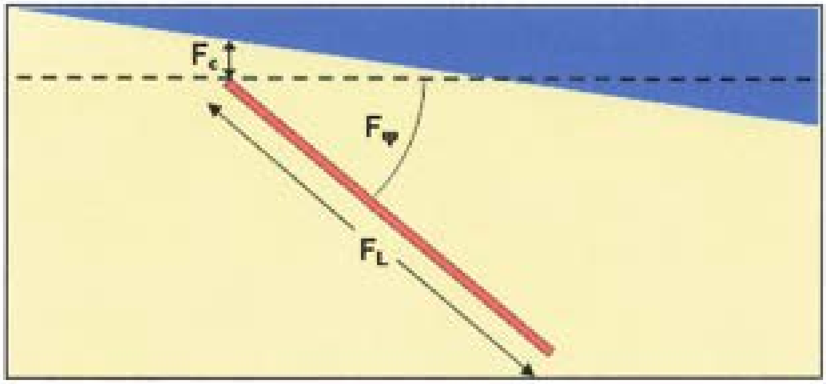

Figure 2-8: Illustration of fracture zone variations. This included varying fracture zone length (F_L), connectivity to lake (F_c) and orientation with respect to horizontal (F_ψ).

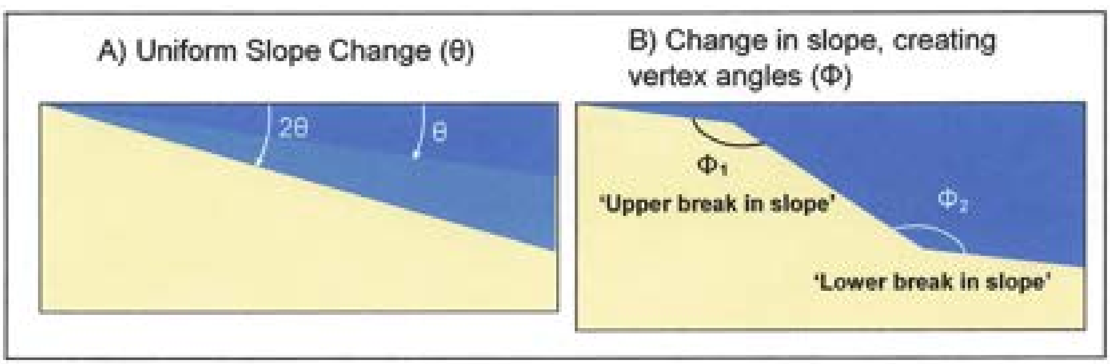

Figure 2-9:
Illustration of lake slope variations. This included A) A uniform change in lake slope (θ) and B) Change(s) in slope, creating a vertex angle (Φ).

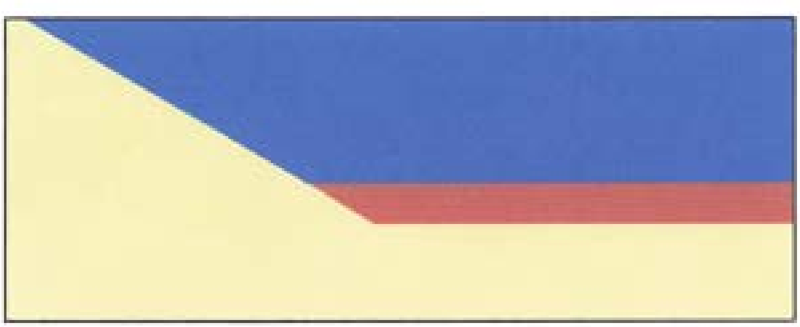

Figure 2-10:
Illustration showing a change in lake slope associated with a change in thickness of lake sediment.

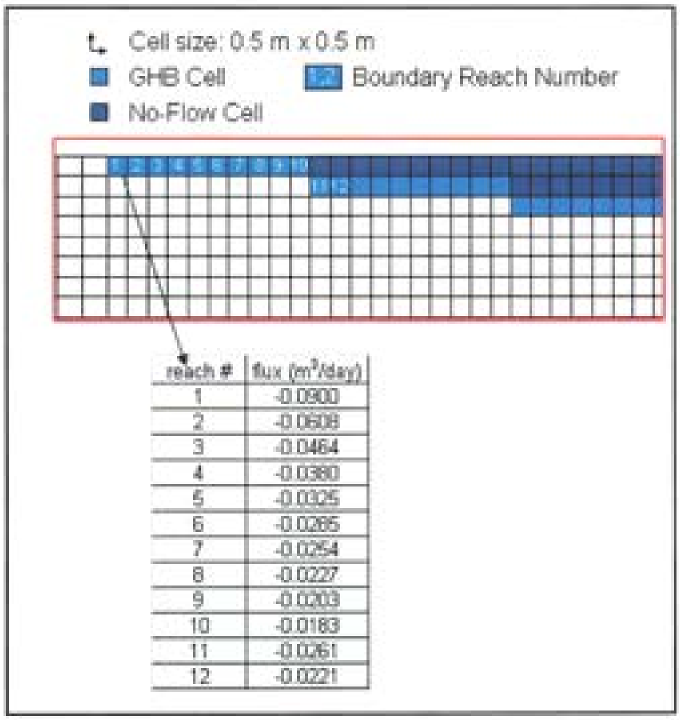

reach #	flux (m³/day)
1	-0.0900
2	-0.0608
3	-0.0464
4	-0.0380
5	-0.0325
6	-0.0285
7	-0.0254
8	-0.0227
9	-0.0203
10	-0.0183
11	-0.0261
12	-0.0221

Figure 2-11: Illustration showing the assignment of reach numbers to each GHB cell and calculated flux values.

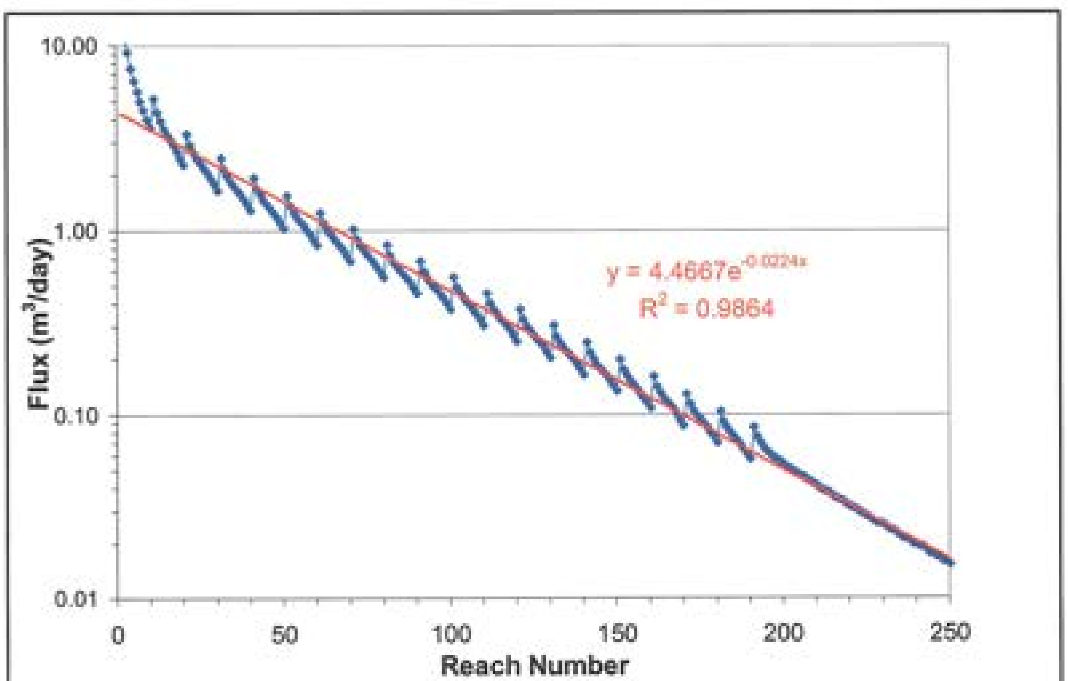

Figure 2-12: Semi-log plot of flux vs. reach number from shore obtained using base-case model conditions. Note the oscillation pattern associated with a finite-difference grid setup. However, the magnitude of oscillation remains roughly the same along each grid row, and thus, the overall trend still exhibits an exponential decline that can fit to an exponential curve.

CHAPTER 3
RESULTS

The results of the model runs are divided into two sections: single-variable model parameters (3.1) and multiple variable parameters (3.2). Single variable parameters, which are discussed first, are parameters that were varied while keeping all other model values constant. These factors are recharge (3.1.1), basin size (3.1.2), aquifer thickness (3.1.3), lake sediment conductance (3.1.4), fracture zone (3.1.5), anisotropy (3.1.6) and lake morphology (3.1.7). Multiple variable parameters, discussed after single-variable parameters, show the effect of combined parameter variation. A change in lake slope was combined with other parameters (3.2.1), including the addition of a coexisting upper break in slope, variable conductance, variable anisotropy, variable aquifer thickness, and sediment heterogeneities. Fracture zone heterogeneities were combined with other parameters (3.2.2), including variable conductance, variable anisotropy, and variable aquifer thickness.

3.1 Single-Variable Model Parameters

3.1.1 Recharge

Varying the base recharge rate (1.13×10^{-3} m/d) uniformly along the top non-lake cells of the model grid had no effect on the distribution of seepage along the lake bottom (Figure 3-1). R^2 values obtained from exponential trends fitted to linear regression for each variation (Table 3-1) were high, and thus, recharge is a factor which does not create non-exponential seepage patterns, at least when it is the only parameter varied. Note that there was little variation in the coefficient β (ranged from -0.0453 to -0.0448) but much variation in the coefficient α (ranged between 0.552

cm/d to 8.519 cm/d). Thus, changing recharge by a factor of x changed total seepage rates by x amount without changing the slope of exponential decline or creating localized seepage peaks.

3.1.2 Basin Size

Like recharge, basin size influenced the overall volume of seepage along a lake without significantly altering the distribution of seepage (Figure 3-2). The coefficient α increased with increasing values L/r (Table 3-2) and there was little variation in the coefficient β (ranged from -0.0463 to -0.0448). Thus, the size of a local groundwater basin controls the volume of water discharging into a lake basin since there is more area for recharge to occur over.

3.1.3 Aquifer Thickness

Aquifer thickness significantly influenced the distribution of seepage in lakes (Figure 3-3). Low b_a/d values forced the majority of seepage to a lake to occur nearshore, while greater values forced seepage further offshore. R^2 values of seepage vs. distance from shore runs for b_a/d values less than 100 were high (Table 3-3), but gradually decreased in value as b_a/d increased. For values greater than $b_a/d = 100$, R^2 is > 0.95, and a slight curvature that departs from linearity is evident. Values of β (ranged between -0.1295 to -0.0097, a factor of 13.5) and values of α for all runs decreased with increasing b_a/d according to a power function with an exponential slope of -0.8 (Figure 3-4), and therefore, the distribution of seepage is very sensitive to small b_a/d ratios but level out when the ratio is greater than 10.

heterogeneity identical in size and hydraulic conductivity will produce a similar relative increase in seepage regardless of its location from shore.

3.1.4.3 Gradual Change Offshore in Conductance

Linearly increasing sediment thickness (b_s) or linearly decreasing sediment conductivity (K_s) gradually from shore resulted in higher seepage rates near shore and lower seepage rates offshore (Figure 3-8) compared with cases of uniform conductance rates ($C = 0.5$ m^2/d, 0.05 m^2/d, and 0.005 m^2/d). A linear increase in sediment thickness produced a curve rather than a line when plotted on a semi-log scale, thus, deviating from an exponential decrease of seepage away from shore (R^2 was > 95). A linear decrease in K_s produced values β of that were nearly identical to β in the case modeling a uniform conductance of 0.5 m^2/d (Table 3-6). Both of these cases, which simulated a 0.5 m^2/d to 0.005 m^2/d change in conductance offshore, produced seepage patterns that differed from the 0.05 m^2/d uniform conductance case, which represents an average between modeled uniform conductances of 0.5 m^2/d and 0.005 m^2/d. Thus, conductance transitions on a large scale (100 m) result in seepage patterns that differ from modeling an equivalent but uniform average conductance.

3.1.5 Fracture Zone Variations

3.1.5.1 Fracture Zone Length and Connectivity to Lake

As the length a fracture zone (F_L) increased, the resulting peak in seepage increased in magnitude as well (Figure 3-9, Table 3-7). A similar effect was seen when fracture zone connectivity to the lake cells (F_c) was varied by increasing the cut-off distance between the termination of the cells assigned as fracture zones and the lake cells. A long fracture (35.5 m to 39.5 m) was used for these model runs, assuming that the length "cut-off" from the fracture zone was minimal compared to the entire length of the fracture zone itself. As the cut-off distance increased, the resulting peak in seepage decreased in magnitude (Figure 3-10, Table 3-8). In addition to decreasing in magnitude, a greater cut-off distance also increased the lake bed area over which the seepage peak was observed, since this cut-off distance allows for flow diverted through the fracture zone to become spread out over a larger portion of the lake bed. Thus, fracture zone length and connectivity can both control the magnitude of a peak in seepage. However, fracture zone connectivity to the lake also influences the area over which preferential flow will become concentrated along a lake bottom.

3.1.5.2 Fracture Zone Distance from Shore

The relative size of a peak in seepage produced by a fracture zone of identical size, orientation, and connectivity varied insignificantly as a function of the distance it was placed from shore (Figure 3-11). Although the magnitude of the peaks increased as the fracture zone was placed closer to shore, the relative size of the peaks remained the same (Table 3-9). Thus, such a heterogeneity will produce a similar relative increase in seepage regardless of its location from shore.

3.1.5.3 Fracture Zone Orientation

In Sections 3.1.5.1 and 3.1.5.2, the fracture zones were situated vertical (parallel to the y-coordinate axis). In the following model runs, the fracture zones were oriented 45°, 90°, 135 °, 153.4°, and 180° with respect to the y-coordinate axis. Head contours from model runs (Figure 3-12) differed significantly depending on fracture zone orientations, which correlated well with the variety of seepage patterns observed (Figure 3-13). Note that the fracture zones oriented most perpendicular to the slope of the lake (90° and 135°) warped head contours to a greater degree than fracture zones oriented more parallel to the slope. The 90° and 135° fracture zone orientations produced the highest, sharpest peaks in seepage, while 45°, 153.4°, and most notably, 180°, produced shallower but broader peaks (Figure 3-12, Table 3-10). Thus, higher, sharper peaks in seepage due to thin fracture zones result when the fracture zone is closer to perpendicular to the slope of the lake, and become shallower and broader in size when oriented closer to parallel to the slope.

3.1.6 Anisotropy

Like sediment conductance and aquifer thickness, varying anisotropy influenced the slope of exponential decline in seepage, β (Figure 3-14). Increasing K_x/K_y decreased β, although linear-regression R^2 values were low (< 0.9) for higher values of K_x/K_y (≥ 20), indicating that an exponential trend does not fit such values of anisotropy well (Table 3-11). When plotted as a function of K_x/K_y, β decreased according to a power function with an exponential slope of -0.287 (Figure 3-15), and therefore, the distribution of seepage offshore is very sensitive to values of K_x/K_y less than 50 but level out when K_x/K_y is greater than 50.

3.1.7 Lake Morphology

3.1.7.1 Uniform Lake Slope

Varying slope (θ) uniformly between 2.86° to 11.3° did not appear to significantly change the distribution of seepage with respect to distance from shore if only the sloped section of the lake is examined, disregarding any offshore break or transition in slope (Figure 3-16).

3.1.7.2 Break in Lake Slope

A break in lake bottom slope produced offshore peaks in seepage that increased in magnitude when the vertex angle (Φ) was increased (Figure 3-17). However, relative the peak increase in seepage for runs between 8.13° to 45° was minimal (increased by factors ranging from 1.35 to 1.74). Thus, a significant break in slope is needed in order to produce a noticeable localized seepage increase.

3.2 Multiple Variable Model Parameters

3.2.1 Lake Slope Morphology Combinations

In the following section, a lake that experiences a lower break in slope of a vertex angle of 26.6° was combined with the addition of a coexisting upper break in slope, variable conductance, variable anisotropy, variable aquifer thickness, and sediment heterogeneities.

An upper and lower break in slope coexisting along a lake bottom produced seepage peaks that were opposite but equal in magnitude (Figure 3-18). The upper break in slope produced a localized minimum at 25 m from shore, transitioning into a localized maximum at 45 m from shore due to the lower break in slope. Thus, whether a break in slope produces a localized minimum versus a localized maximum depends on if the transition at the vertex angle is from a shallower slope to a steeper slope (upper break in slope example) or from a steeper to a shallower slope (lower break in slope example).

Varying sediment conductance between C = 1 to C = 0.02 influenced the size of the peak produced by the 26.6° break in slope (Figure 3-19). The relative size of the peak was reduced by a factor of 2 when conductance decreased by only a small amount (one order of magnitude), indicating that low-K lake sediment buffers the effects of slope variations on seepage patterns by redistributing flow more evenly along the lake. Varying the aquifer thickness to lake depth ratio, b_a/d, had little effect on magnifying or reducing the size of the peak produced by the 26.6° break in slope (Figure 3-20).

Increasing anisotropy (K_x/K_y) within an aquifer near a lake that experiences a break in slope increased the size of the peak produced by the break in slope (Figure 3-21). Note also that increasing anisotropy resulted in more seepage concentrated along the slope section of the lake (first 20 m from shore) and less concentrated further away from shore along the flat section of the lake. Thus, lake morphology patterns can create significant deviations in the distribution of seepage along a lakebed if anisotropic conditions exist within the surrounding aquifer, but are not significant when only isotropic conditions exist.

A 26.6° break in lake slope due to a pinch-out in sediment thickness produced a 143x magnification in seepage at that location compared with the same break in slope by itself, which only produced a 1.31x magnification in seepage (Figure 3-22). Furthermore, when the same sediment pinch-out pattern was moved closer to shore away from the break in slope, a significant change in seepage (123x) still occurred. Thus, a pinch-out due to a break in slope produced a peak in seepage that was only slightly larger (1.2x) then the peak produced by the same pinch-out alone.

3.2.2 Fracture Zone Combinations

In the following section, a fracture zone with a conductivity 100x that of the surrounding porous medium with constant in length, connectivity to shore, distance from shore, and orientation was combined with variable conductance, variable anisotropy, and variable aquifer thickness.

Increasing sediment conductance significantly reduced the size of a peak produced by the high-K fracture zone (Figure 3-23). Note that values of C lower than 0.01 m^2/d were not modeled since the size of the peak was reduced to close to the (homogeneous) base case. Unlike a break in slope combined with anisotropic conditions, varying K_x/K_y did not significantly magnify or reduce the peak in seepage produced by a high-K fracture zone (Figure 3-24). Aquifer thickness variations also had little effect on reducing or increasing the magnitude of the peak produced by a high-K fracture zone (Figure 3-25). However, note that increasing aquifer thickness resulted in a reduced seepage rate observed at the peak in seepage, although such a change is observed also in seepage rates surrounding the fracture zone due to the decrease in the exponential slope of seepage caused by increasing aquifer thickness.

3.3 Summary

Two-dimensional models of groundwater discharge to lakes revealed different patterns of seepage from varying hydrogeologic factors. By using modeling, the relative influence of different factors could be evaluated. One of the most important factors was the presence of low-K lake sediment. A localized thinning of low-K lakebed sediments produced the largest peaks in seepage, and low-K lakebed sediments positioned above either a high-K fracture zone or a break in lake slope significantly reduced the size of the peak produced by these parameters without the lake sediment. Lower lakebed conductance closer to shore increased seepage there, changing the degree of exponential decline. Although high aquifer anisotropy (K_x/K_y)

had little influence on the size of a peak produced by a fracture zone, it greatly magnified the size of a peak produced by a break in lake slope.

In addition to factors producing peaks in seepage, other factors influenced the slope of exponential decline of seepage away from shore, the total volume of seepage in a lake, or had little or no influence on changing seepage patterns. These are discussed further in the next section.

Table 3-1: Various recharge (percent of precipitation) variations with respective α, β, and R^2 values obtained from linear regression analysis.

Recharge (% of Precipitation)	α	β	R^2
0.042	0.552	-0.0449	0.9936
0.083	1.083	-0.0450	0.9962
0.167	2.173	-0.0453	0.9966
0.333	4.245	-0.0448	0.9971
0.667	8.519	-0.0449	0.9971

Table 3-2: Various basin size (L/r) variations with respective α, β, and R^2 values obtained from linear regression analysis.

L/r	α	β	R^2
7	7.471	-0.0449	0.9971
5	5.310	-0.0448	0.9971
4	4.245	-0.0448	0.9971
3	3.225	-0.0451	0.9968
2	2.166	-0.0452	0.9966
1	1.149	-0.0463	0.9931

Table 3-3:
Various aquifer thickness (b_a/d) variations with respective α, β, and R^2 values obtained from linear regression analysis Note that for high values of b_a/d, R^2 values are low, indicating that seepage with distance from shore does not follow an exponential trend as well as those with low values.

b_a/d	α	β	R^2
1.50	12.33	0.1295	0.9936
1.75	11.03	0.1128	0.9903
1.85	10.21	0.1058	0.9927
2.00	9.16	0.0969	0.9969
2.25	8.93	0.0868	0.9966
2.50	7.74	0.0771	0.9975
2.75	7.03	0.0702	0.9974
3.00	6.35	0.0641	0.9977
3.50	5.49	0.0552	0.9967
4.00	4.56	0.0475	0.9972
5.00	3.50	0.0374	0.9950
6.00	2.92	0.0313	0.9907
7.50	2.42	0.0257	0.9823
10.00	1.95	0.0206	0.9650
12.50	1.68	0.0176	0.9453
15.00	1.51	0.0157	0.9273
20.00	1.29	0.0133	0.8943
25.00	1.16	0.0119	0.8648
35.00	1.04	0.0105	0.8210
50.00	0.98	0.0097	0.7938

C (m^2/d)	β	R^2
1.00E+00	0.0448	0.9971
6.40E-01	0.0447	0.9969
3.20E-01	0.0437	0.9972
1.60E-01	0.0419	0.9978
1.00E-01	0.0399	0.9983
8.00E-02	0.0386	0.9985
5.00E-02	0.0354	0.9989
4.00E-02	0.0337	0.9990
2.50E-02	0.0296	0.9992
2.00E-02	0.0275	0.9993
1.00E-02	0.0212	0.9993
5.00E-03	0.0156	0.9994
2.50E-03	0.0109	0.9997
1.25E-03	0.0073	0.9998
1.00E-03	0.0063	0.9998
1.00E-04	0.0009	0.9967
1.00E-05	0.0001	0.9955

Table 3-4: Various GHB conductances (m^2/d) with respective β and R^2 values obtained from linear regression analysis. If 0.5 m thick sediment is assumed, the model value of C (m^2/d) is equal to sediment K (m/d). Note that R^2 values are high, indicating that these runs fit an exponential trend well. Decreasing conductance increased the contrast in hydraulic conductivity between lake sediments and the aquifer, resulting in seepage being spread more uniformly across the lake bottom as this contrast increased.

pinch-out %	M
100.0	145.7
99.5	106.8
95.0	18.3
75.0	3.9
50.0	2.0
0.0	1.0

Table 3-5: List of modeled pinch-out percentages and the relative change in seepage (M) produced by each peak.

Table 3-6:

β obtained from linear regression analysis for models of gradually increasing sediment thickness and conductivity. Note that β in the uniform case C=0.05 is lower in value than either of the gradual sediment change cases.

Sediment Configuration	β	R^2
C=0.5 (uniform)	-0.0443	0.9865
C=0.05 (uniform)	-0.0349	0.9961
C=0.005 (uniform)	-0.0149	0.9999
Linear Decrease in K_s	-0.0431	0.9834
Linear Increase in b_s	-0.0399	0.9441

F_L	M
24.5	7.1
12.0	5.4
8.0	4.0
4.0	2.6
0.0	1.0

Table 3-7: List of fracture zone length (m) variations and the relative change in seepage (M) produced by each peak.

F_c	M
0.0	7.1
0.5	4.3
1.0	3.2
2.0	2.2
4.0	1.5

Table 3-8: List of fracture zone connectivity (m) variations and the relative change in seepage (M) produced by each peak.

Fracture Zone (mfs)	M
22.75	4.308
37.75	4.384
52.75	4.368
67.75	4.341

Table 3-9: List of fracture zone distance from shore (m) variations and the relative change in seepage (M) produced by each peak.

F_ψ	M
45.0	3.0
90.0	4.9
116.6	4.9
135.0	4.6
153.4	3.7
180.0	2.0

Table 3-10: List of fracture zone orientation (degrees) variations and the relative change in seepage (M) produced by each peak.

Kx/Ky	β	R^2
1	-0.0447	0.9866
2	-0.0342	0.9726
5	-0.0254	0.9461
10	-0.0206	0.9220
20	-0.0170	0.8945
50	-0.0129	0.8461
100	-0.0105	0.7965
200	-0.0088	0.7368
500	-0.0078	0.6934

Table 3-11: β obtained from linear regression analysis for anisotropy (K_x/K_y) variations. Note that R^2 was low (< 0.95) for values of $K_x/K_y > 5$, indicating that an exponential trend does not fit such values of K_x/K_y well.

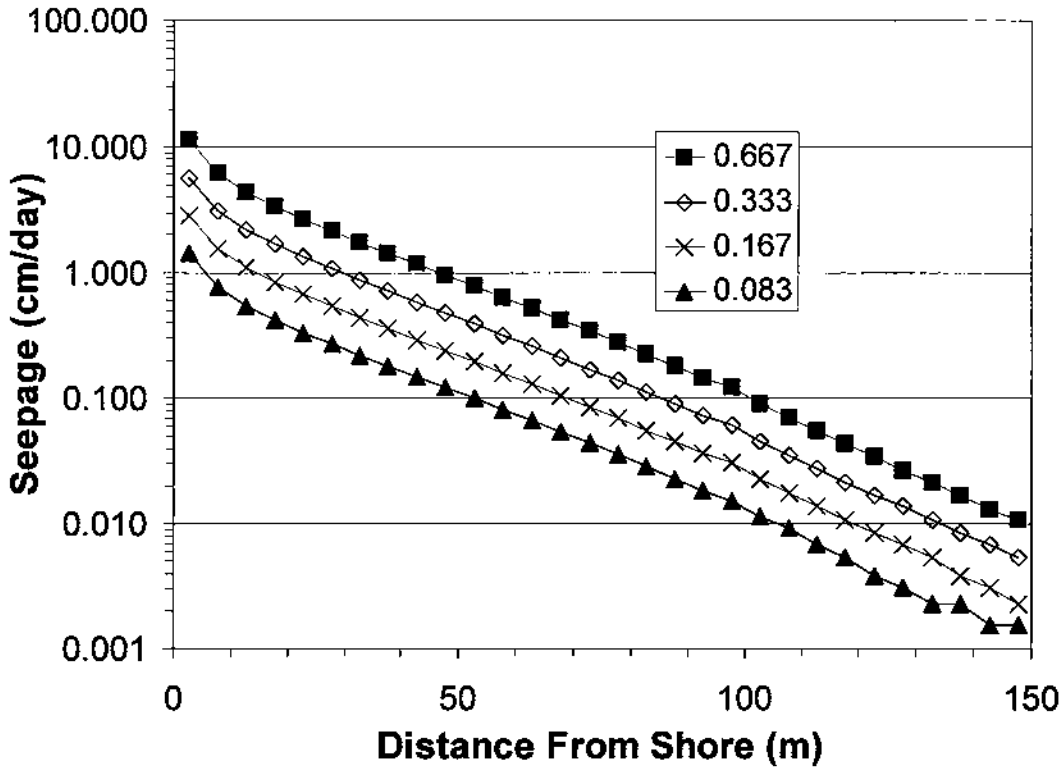

Figure 3-1: Semi-log seepage vs. distance from shore plot of four modeled recharge (percent of precipitation) variations. Note that recharge has little influence on the slope of exponential decline but is more important in increasing or reducing overall seepage to a lake.

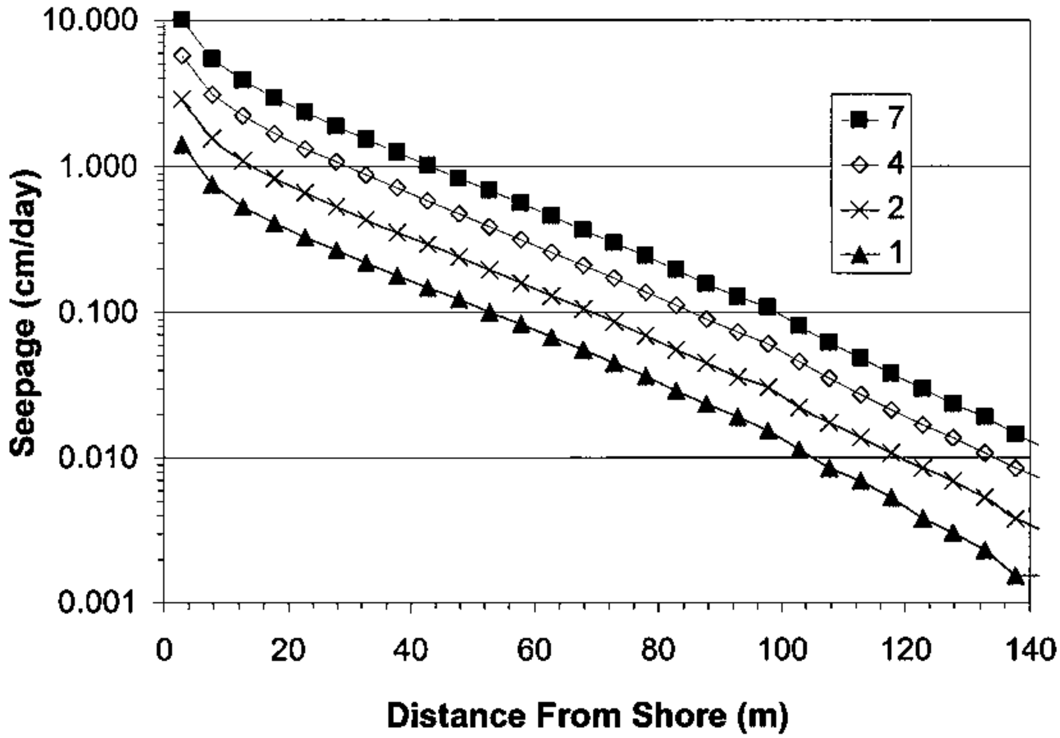

Figure 3-2:
Semi-log seepage vs. distance from shore plot of three modeled basin size (L/r) variations. Like recharge, basin size has a strong influence in increasing/decreasing overall seepage rates without significantly influencing the distribution of seepage along the lake.

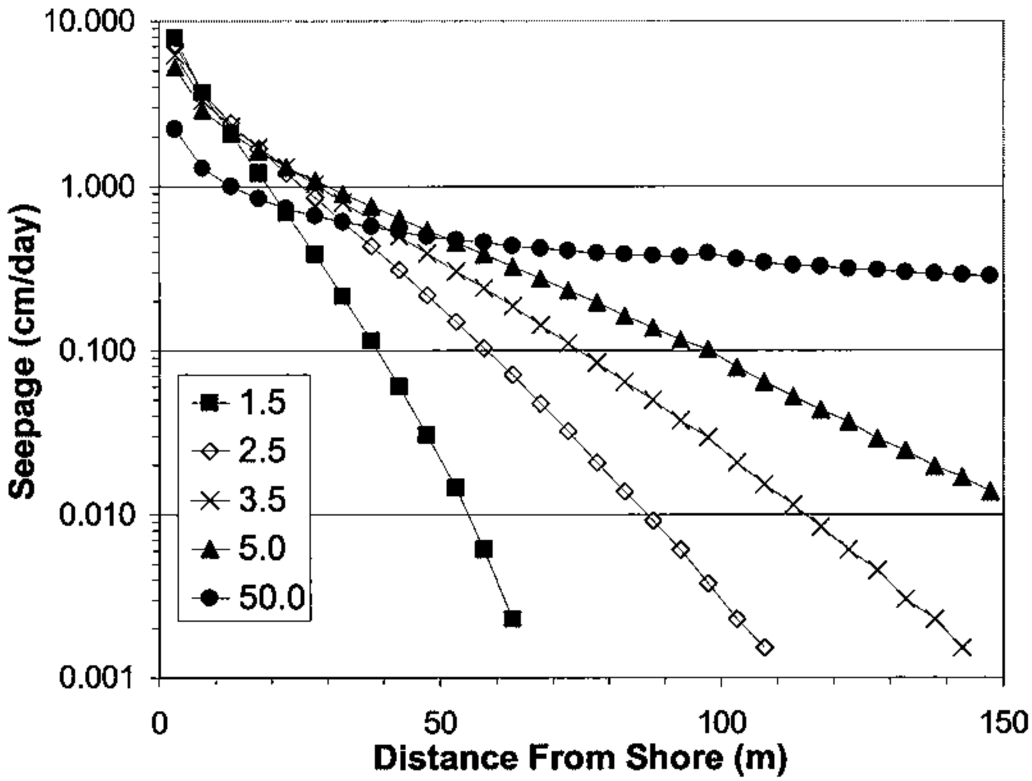

Figure 3-3:
Semi-log seepage vs. distance from shore plot of five modeled aquifer thicknesses (b_a/d) variations. Seepage was distributed close to shore when b_a/d values were low, but spread out further from shore as b_a/d values increased.

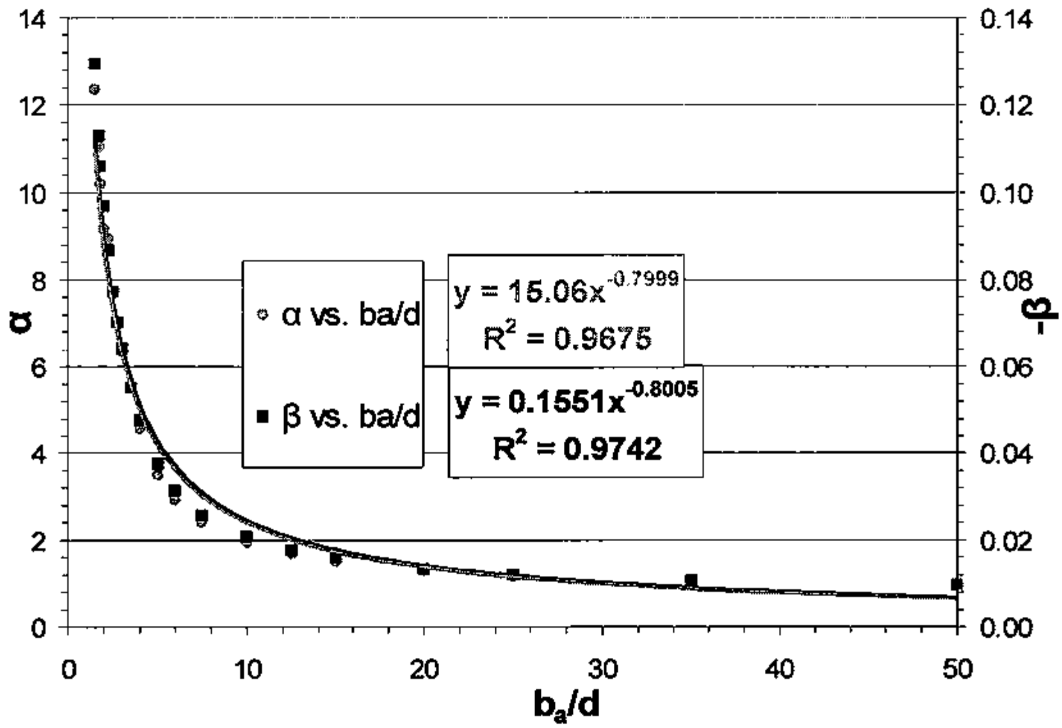

Figure 3-4: Plot of α and -β vs. b_a/d values obtained from Table 3.2. –β rather than β was plotted in order to fit an exponential trend line to the data. Note that both of these coefficients decreased according to a power function with a slope of -0.8. Thus, α ~ (b_a/d)-0.8 and β ~ -(b_a/d)-0.8.

3.1.4 Lake Sediment

3.1.4.1 Uniform Lake Sediment Conductance

Decreasing lake sediment conductance distributed seepage rates more evenly across the lake to a further degree than aquifer thickness variations (Figure 3-5). The slope of exponential decline (β) ranged between -0.0448 and -0.0001, a factor of 450 (Table 3-4). As a function of conductance, β changed most rapidly when conductance was modeled between 0.1 m^2/d to 0.001 m^2/d (Figure 3-6). β appears to level off as sediment conductance approaches base conductance ($C = 1\ m^2/d$) and for values lower than 0.001 m^2/d. Thus, sediment conductance rates < 0.1 m^2/d begin to strongly reduce the slope of exponential decline, but level off asymptotically, since this slope can never reach zero, and therefore, conductance rates < 0.001 m^2/d essentially distributes seepage evenly across a lakebed.

3.1.4.2 Localized Lake Sediment Heterogeneity

Pinch-out variations produced single non-exponential peaks in seepage that increased in magnitude as the sediment pinch-out percentage increased (or as the contrast in conductance increased) (Figure 3-7). The relative size of this peak (M) also increased as the pinch-out percent increased, especially when modeled at 95% or greater (Table 3-5). For a 95% pinch-out M was 18, and in the full pinch-out model, seepage rates increased in comparison to surrounding seepage rates by 146x (M = 146). The relative peak magnitude produced by a 100% pinch-out varied insignificantly as a function of the distance it was placed from shore (Figure 3-7). Although the magnitude of the peaks increased as the pinch-out was placed closer to shore, the relative size of the peaks remained the same. Thus, a geologic

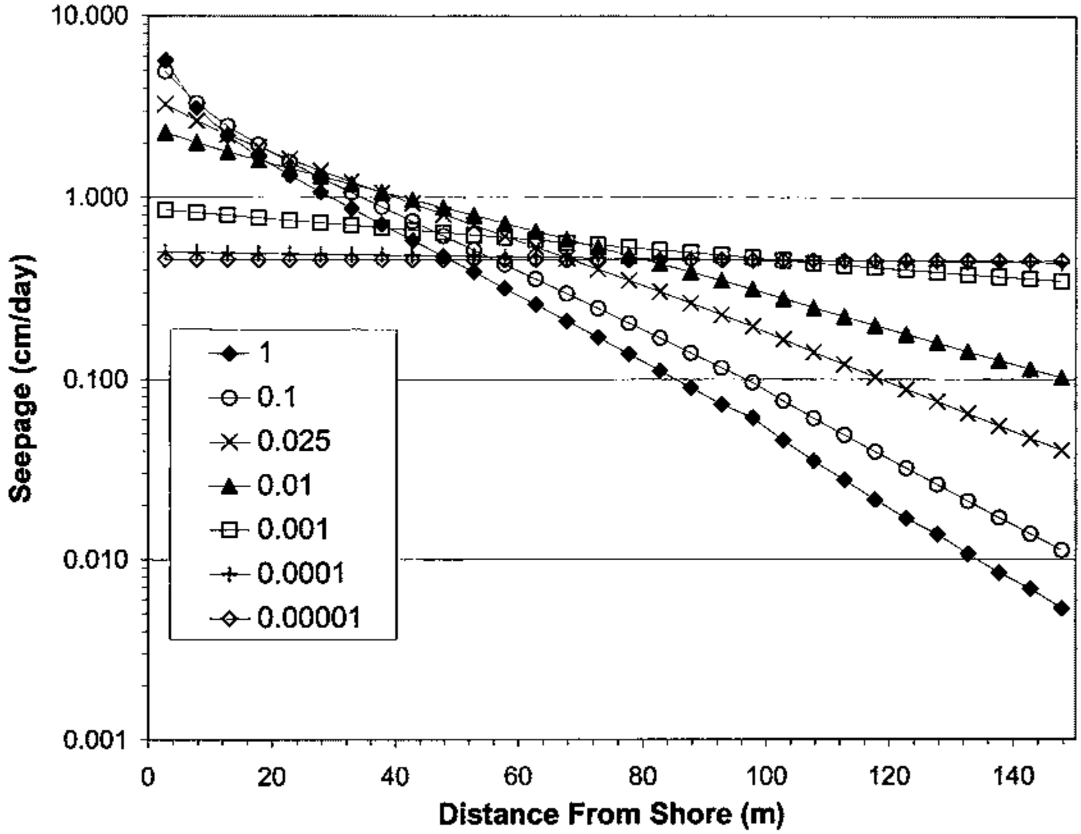

Figure 3-5:
Semi-log seepage vs. distance from shore plot of seven modeled GHB sediment conductance (m^2/d) variations. Decreasing the conductance of the GHB cells resulted in a more even distribution of seepage along a lake, thus, reducing the slope of exponential decline. For very low conductance values this slope approached but did not reach zero, a case in which seepage would be distributed at a uniform rate with respect to distance from shore.

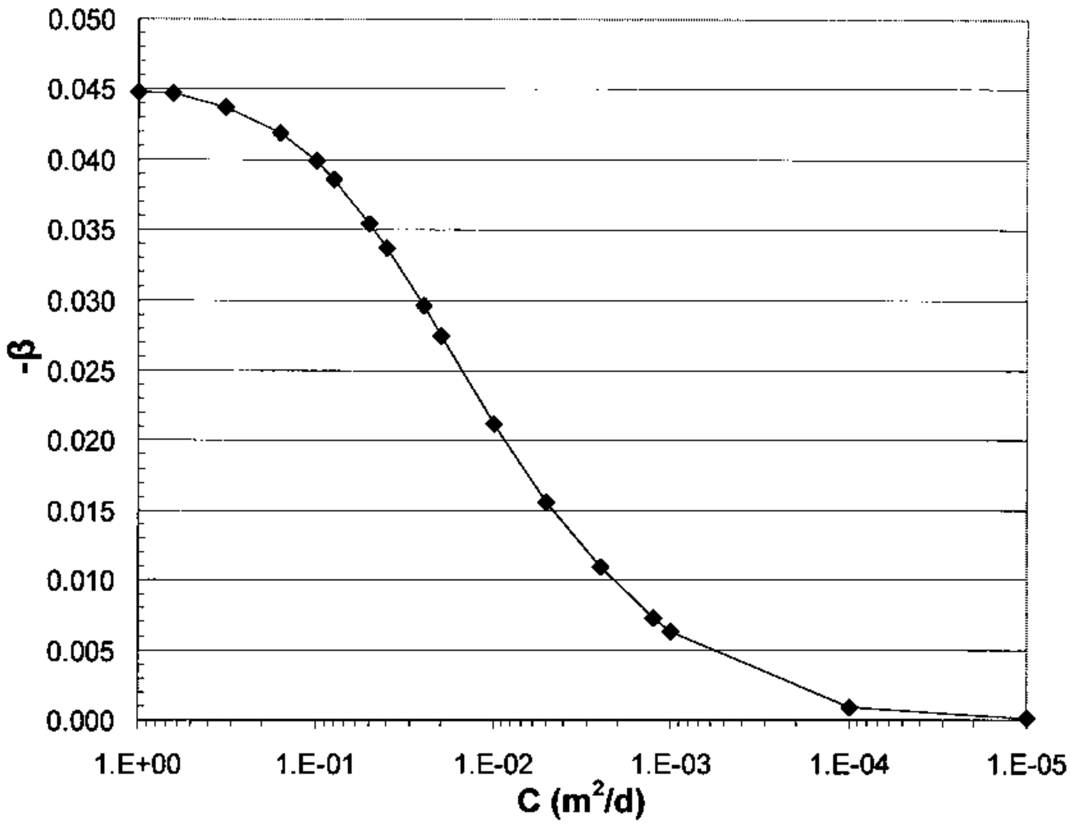

Figure 3-6:
Semi-log plot of β vs. GHB conductance (m^2/d) variations. β changed most rapidly when conductance was modeled between 0.1 m^2/d to 0.001 m^2/d, but appears to level off as sediment conductance approaches base conductance (C = 1 m^2/d) and for values lower than 0.001 m^2/d.

A)

B)

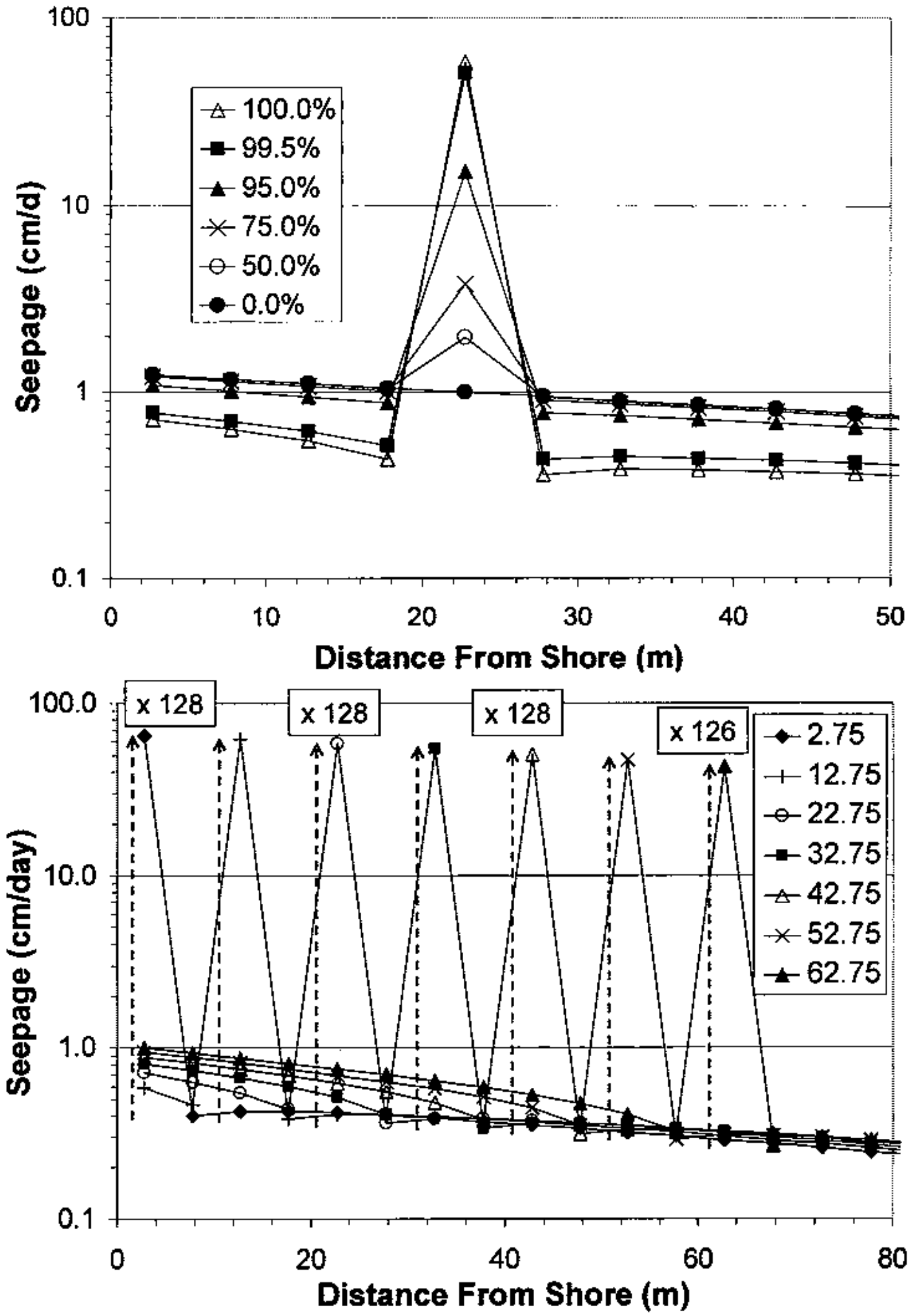

Figure 3-7:
A) Semi-log seepage vs. distance from shore plot of six modeled localized sediment heterogeneities. These heterogeneities, expressed as a percent of sediment pinch-out, produced peaks in seepage, which increased in magnitude as the sediment became thinner (or as the contrast in conductance increased). **B)** Semi-log seepage vs. distance from shore plot of seven identical localized sediment heterogeneities placed at various distances (m) from shore. Note that the relative size of the peaks is constant, although the magnitude of the peaks decreases away from shore.

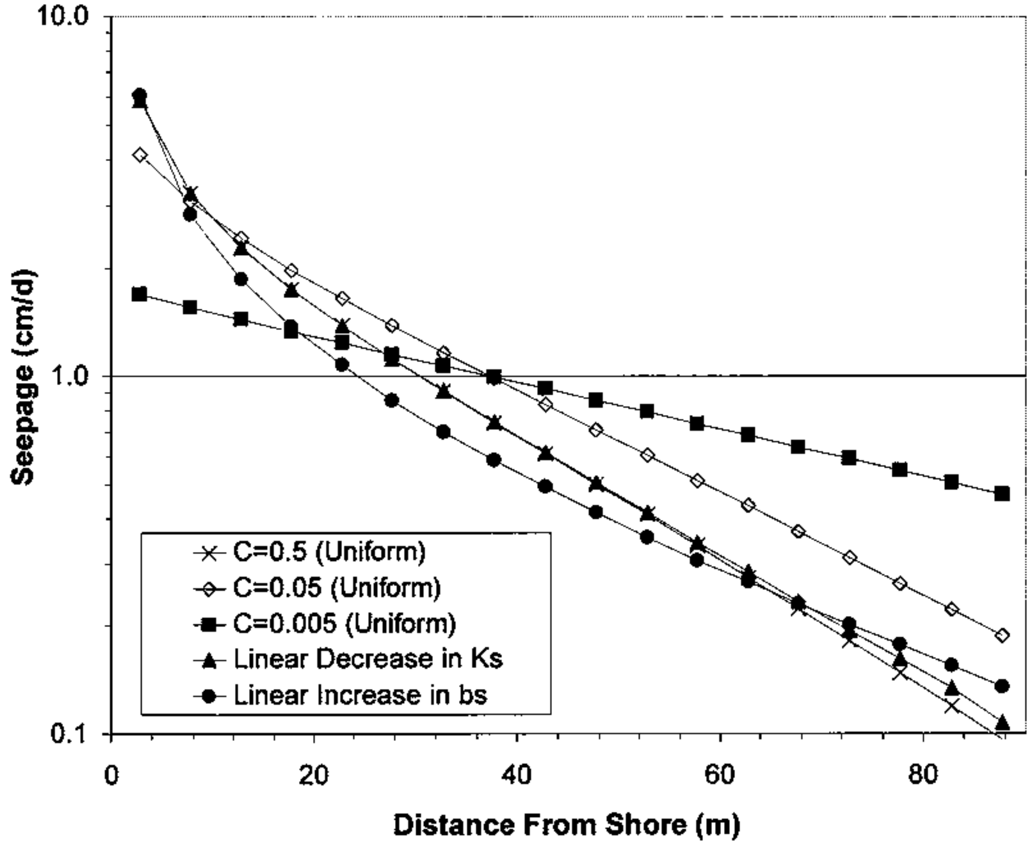

Figure 3-8:
Semi-log plot of seepage vs. distance from shore for models of gradually increasing sediment thickness and conductivity.

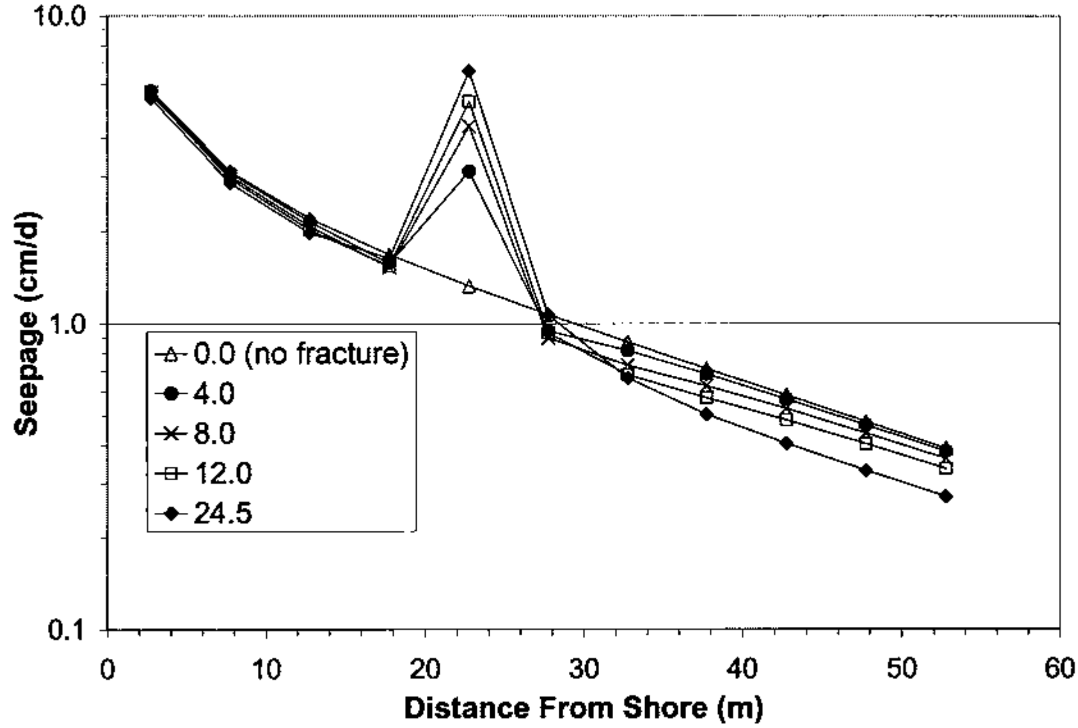

Figure 3-9: Semi-log plot of seepage vs. distance from shore for fracture zone length (m) variations. All fracture zones modeled were zoned with a conductivity 100x that of surrounding non-fracture zone cells. Note that increasing the fracture zone length increased the magnitude of the seepage peak.

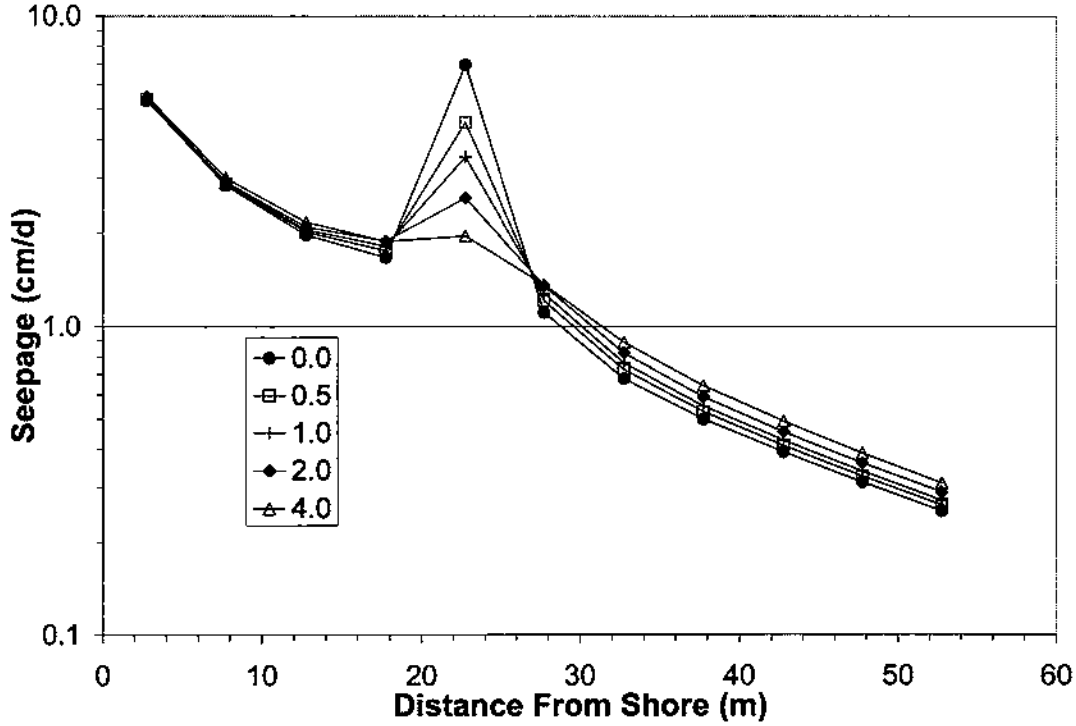

Figure 3-10: Semi-log plot of seepage vs. distance from shore for fracture zone connectivity (m) variations. Note that increasing this distance decreased the magnitude of the seepage peak.

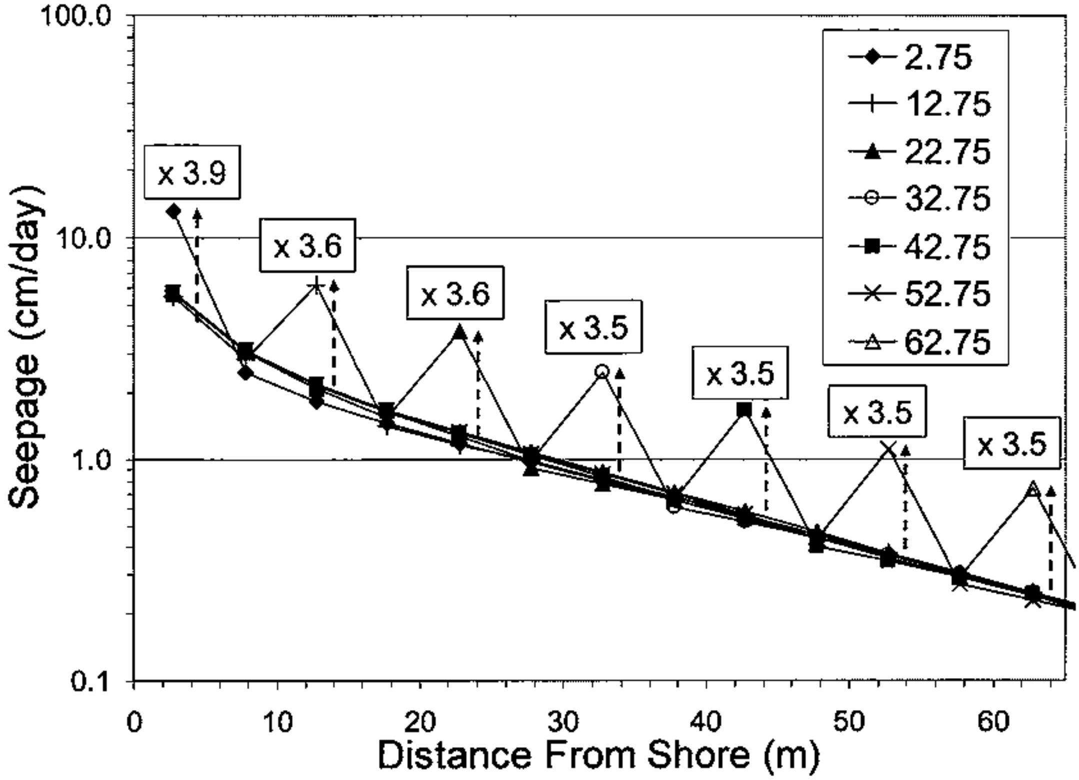

Figure 3-11: Semi-log plot of seepage vs. distance from shore for a fracture zone placed at various distances (m) from shore. Note that although the magnitude of this peak decreased in value as the fracture zone was modeled away from shore, but the relative size of the peak (shown above each model run) remained relatively constant.

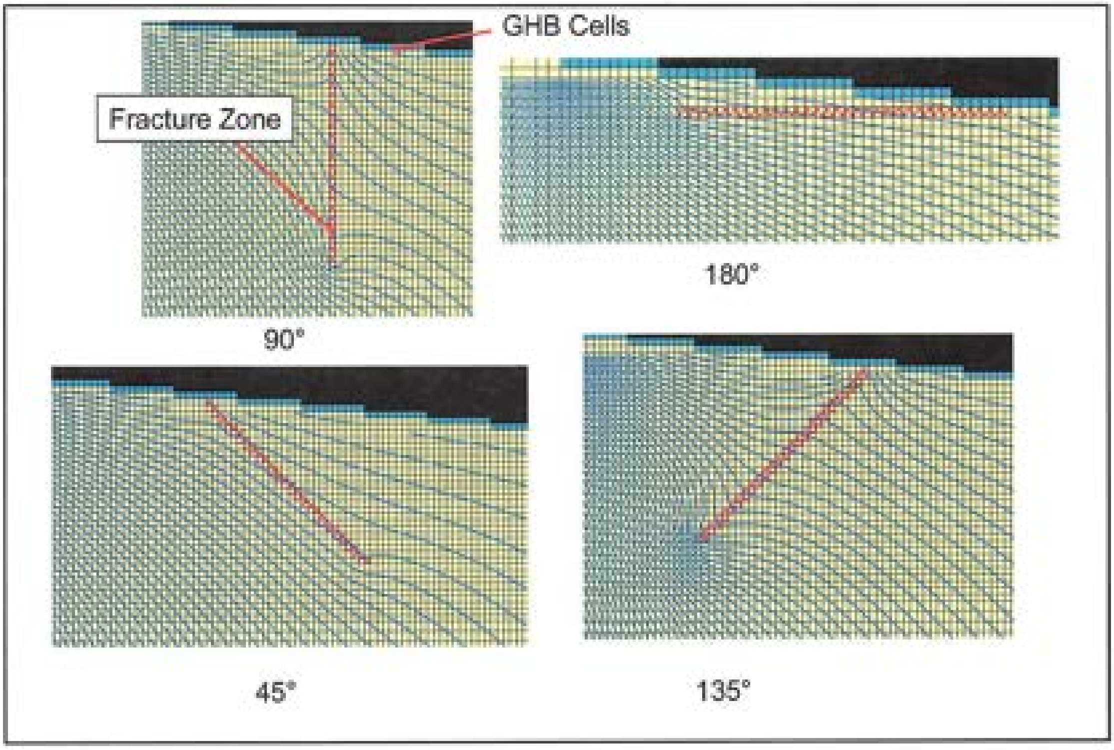

Figure 3-12:
Model diagrams illustrating the effect of fracture zone orientation on contour heads (1 cm intervals). Note that the fracture zones oriented closer to parallel to the general direction of flow below the lake (90° and 135°) seem to cause more significant deviations in head contours.

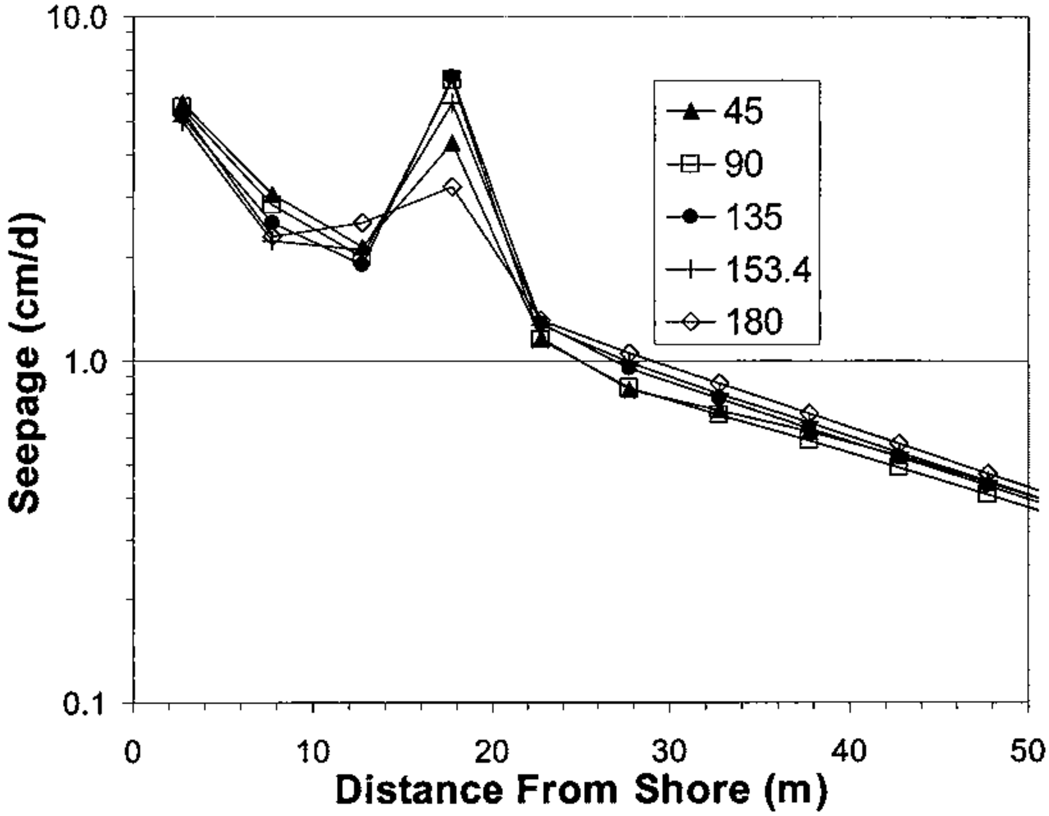

Figure 3-13:
Semi-log plot of seepage vs. distance from shore for five fracture zone orientation (degrees) variations . Note that the 90° and 135° orientations produced the highest, sharpest peaks while the 0°, 45°, and 153.4° orientations produced shallower, broader peaks.

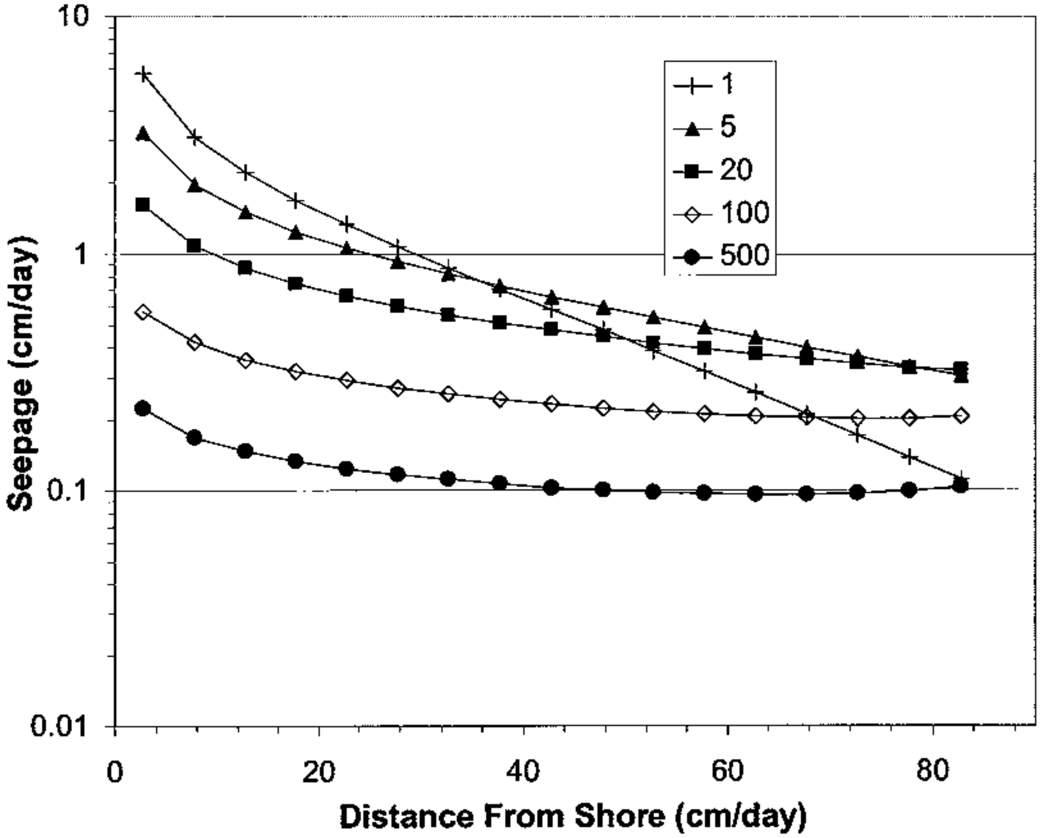

Figure 3-14:
Semi-log plot of seepage vs. distance from shore for the five anisotropy (K_x/K_y) variations . Note that increasing K_x/K_y distributes seepage more evenly across a lakebed.

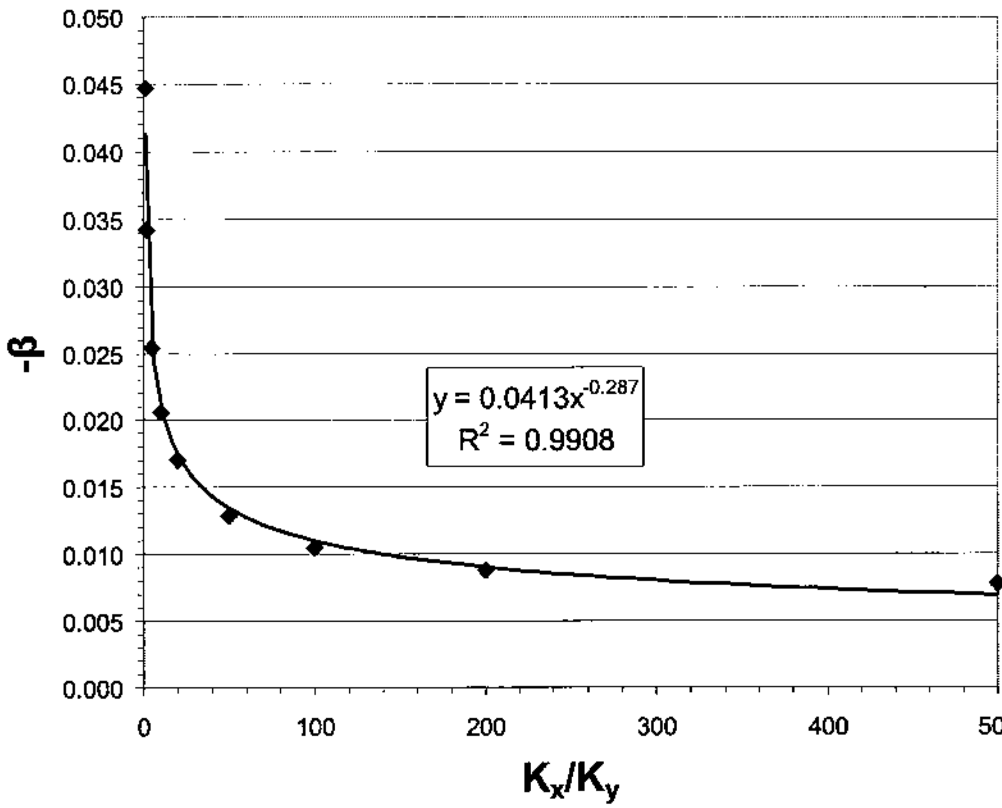

Figure 3-15:
β vs. K_x/K_y obtained from data in Table 3-6. β decreased according to a power function with an exponential slope of -0.287 and therefore, the distribution of seepage offshore is very sensitive to values of K_x/K_y less than 50 but level out when K_x/K_y is greater than 50.

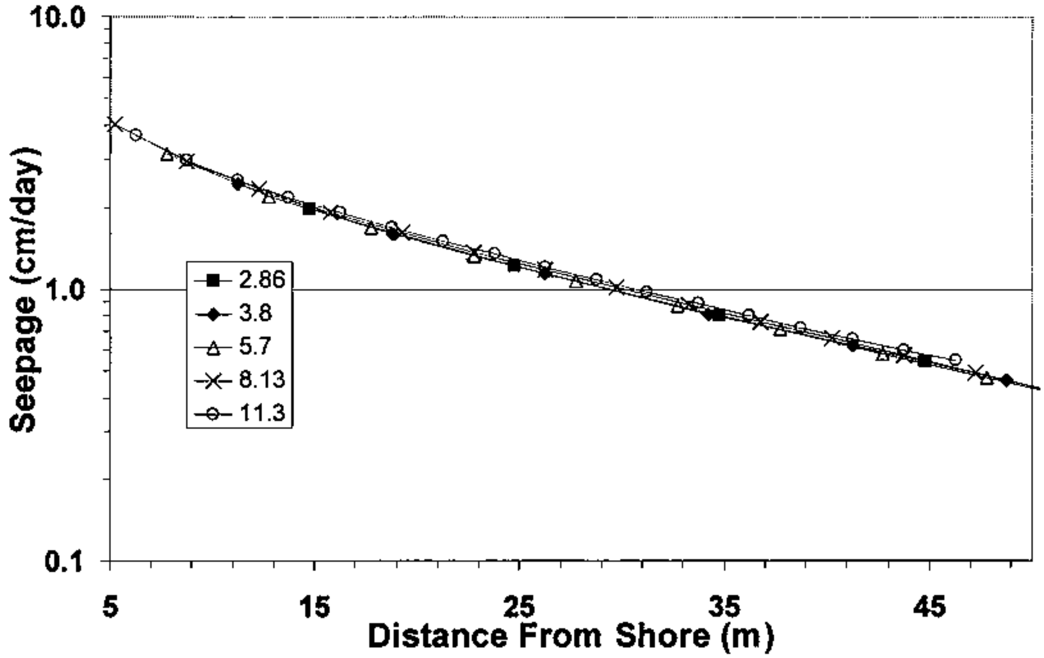

Figure 3-16: Semi-log plot of seepage vs. distance from shore for various uniform slope (degrees) variations. Note that varying the degree of this slope had little influence on the distribution of seepage.

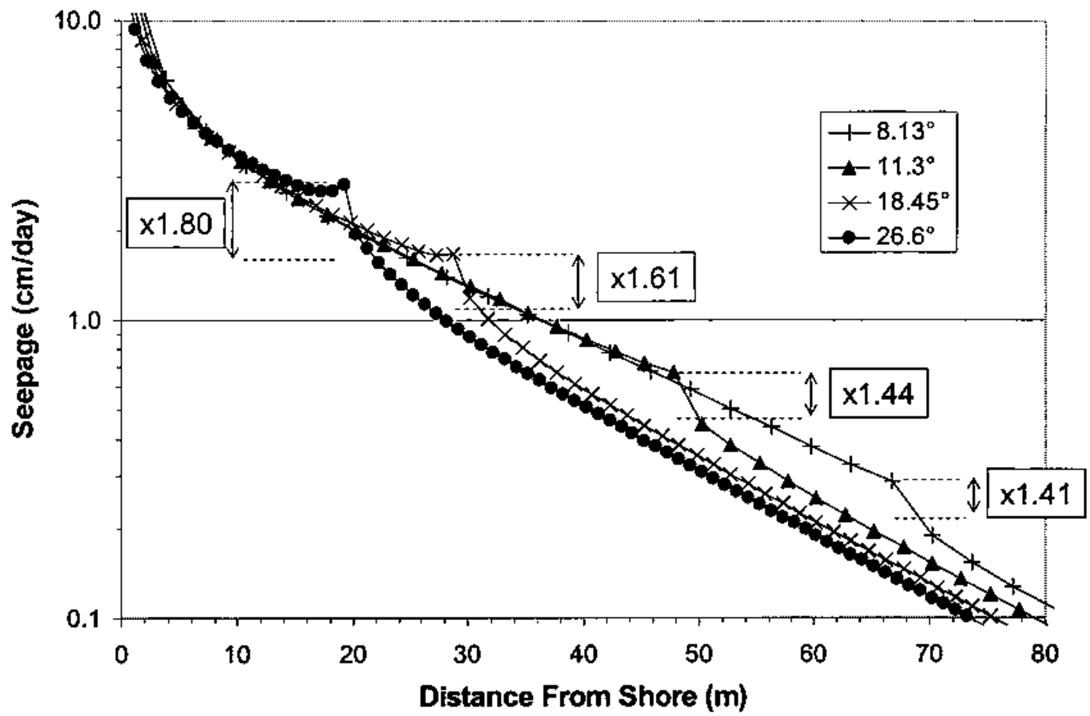

Figure 3-17: Semi-log plot of seepage vs. distance from shore for various vertex angles (degrees) at a break in lake slope. The relative size of the seepage peak (M) for each modeled vertex angle is also shown. Note that a significant break in slope is needed to create even a slight peak in seepage.

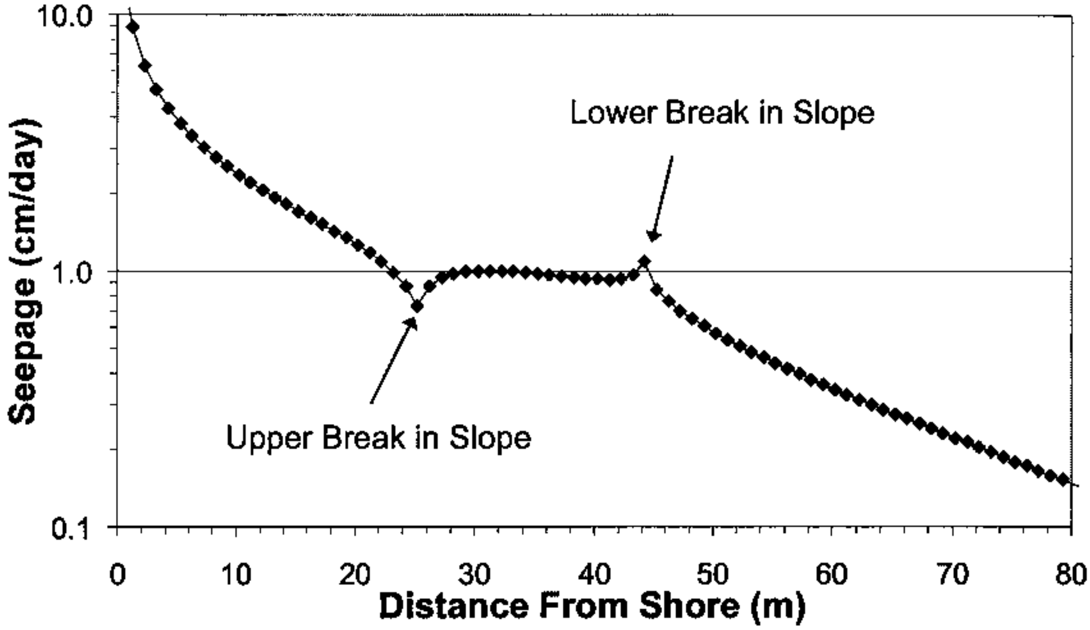

Figure 3-18: Semi-log plot of seepage vs. distance from shore of an upper and lower break in slope both with a vertex angle of 26.6°. Note that the features produced peaks that were opposite but equal in magnitude.

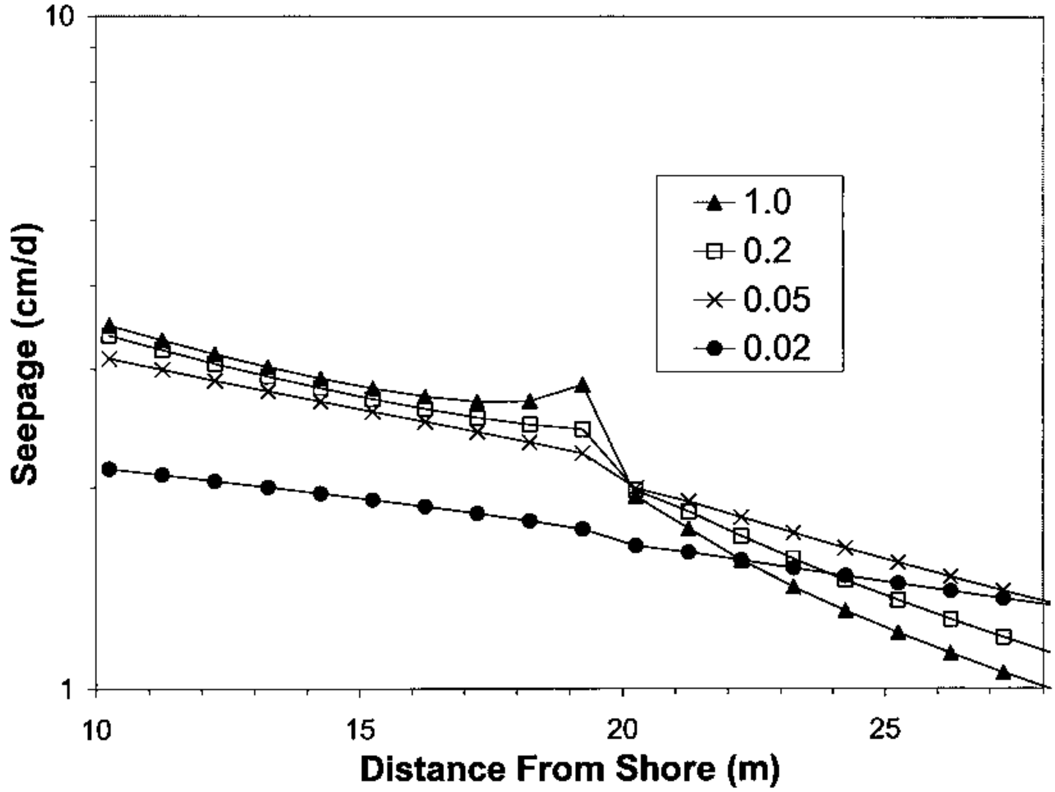

Figure 3-19: Semi-log plot of seepage vs. distance from shore of a 26.6° break in slope combined with variable lake sediment conductance (m^2/d). Note that decreasing conductance decreased the size of the peak produced by the break in slope.

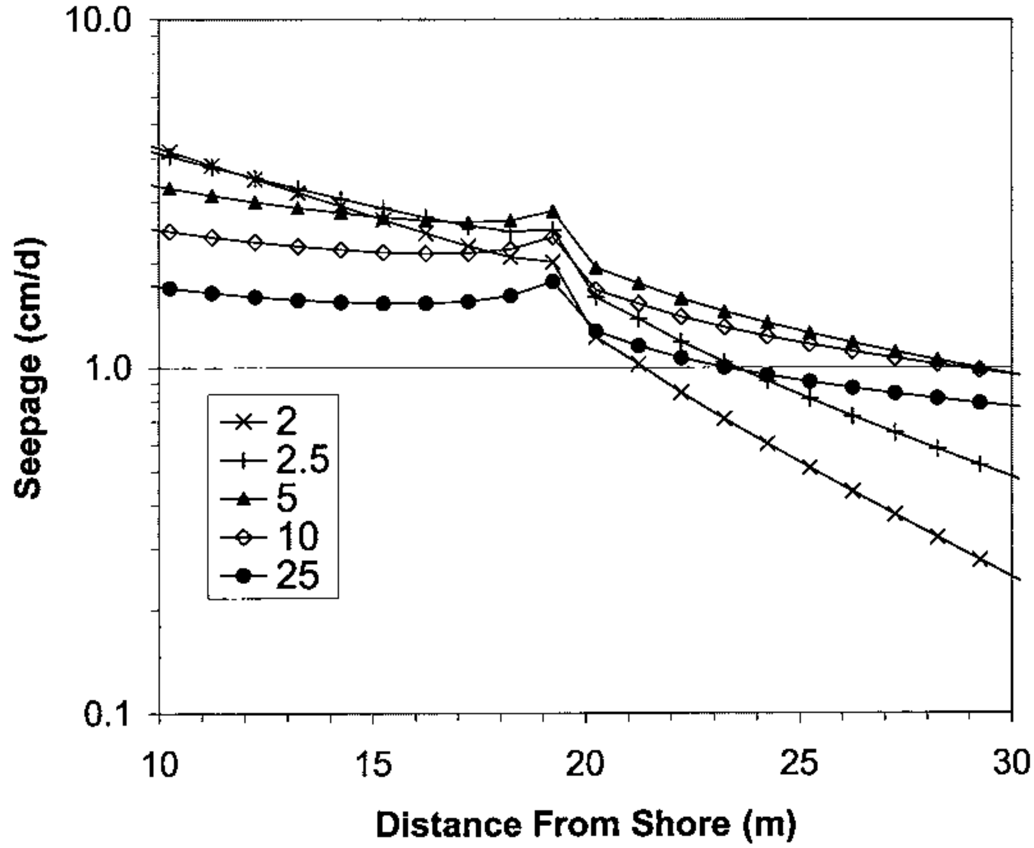

Figure 3-20: Semi-log plot of seepage vs. distance from shore of a 26.6° break in slope combined with variable aquifer thickness (b_a/d). Note that varying this parameter had little effect on magnifying or reducing the size of the peak produced by the break in slope.

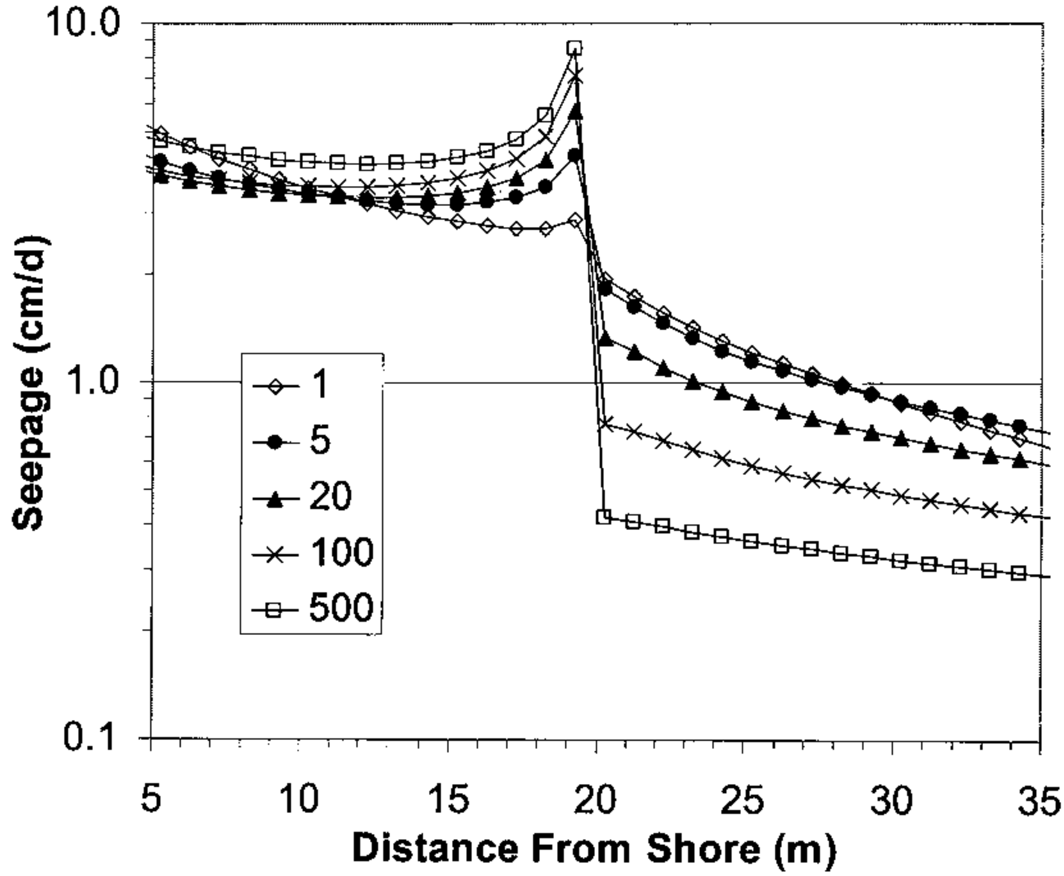

Figure 3-21: Semi-log plot of seepage vs. distance from shore of a 26.6° break in slope combined with variable anisotropy (K_x/K_y). Note that increasing anisotropy significantly increased the size of the peak produced by the break in slope and also that the seepage diverted to the sloped section of the lake greatly exceeds that diverted to the flatter section of the lake that begins 20 m from shore.

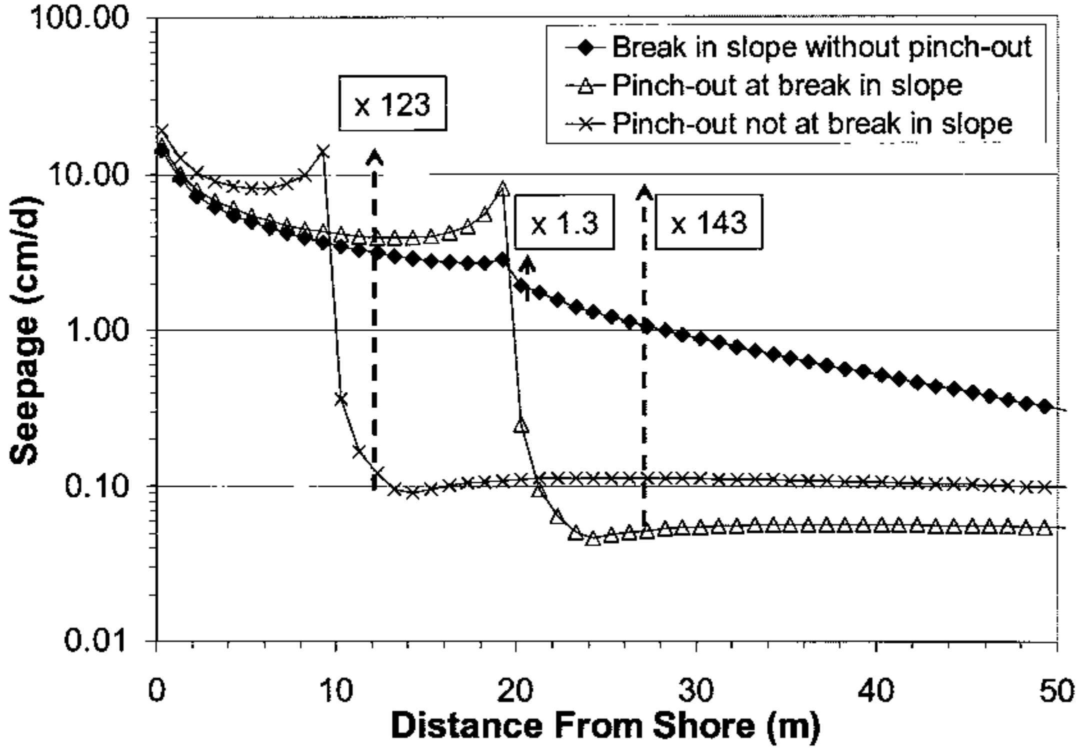

Figure 3-22: Semi-log plot of seepage vs. distance from shore of a pinch-out in sediment thickness combined with a break in slope. A sediment pinch-out alone placed closer to shore and the break in slope without the pinch-out are also shown for comparison. Note that the seepage peak produced by the pinch-out heterogeneity significantly outweighs that produced by the break in slope alone and is not significantly higher when placed alongside the break in slope.

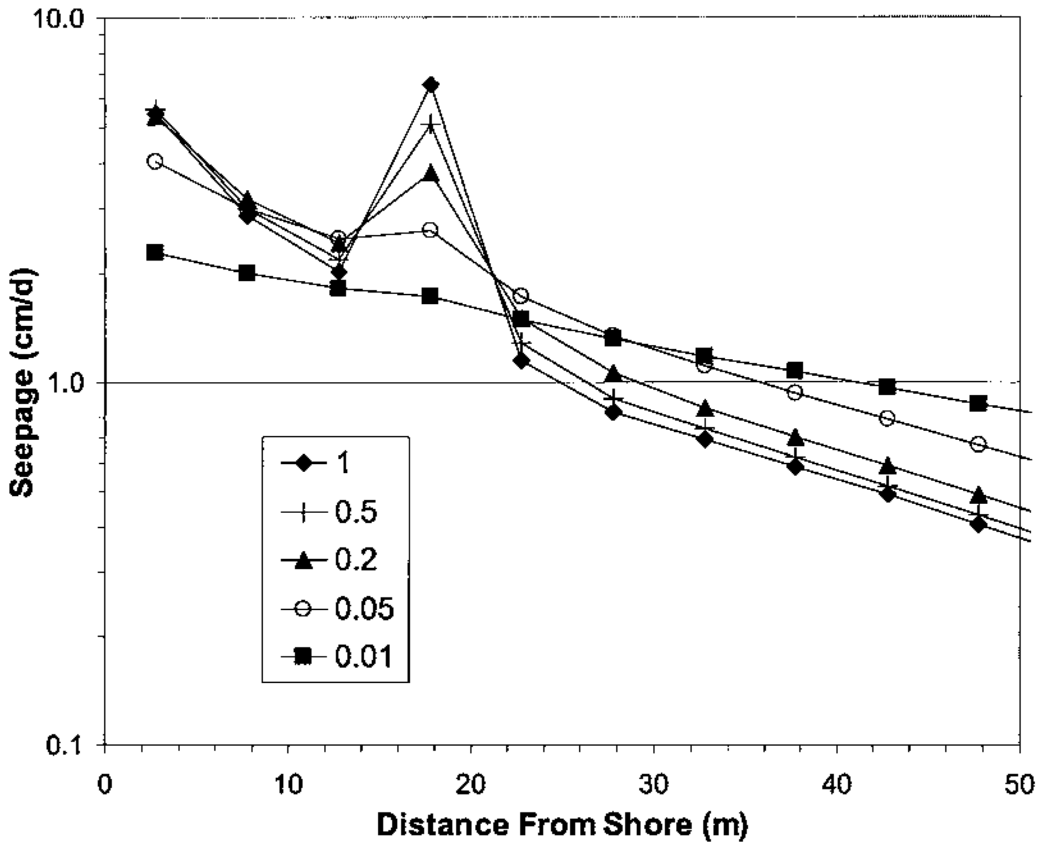

Figure 3-23: Semi-log plot of seepage vs. distance from shore of a high-K fracture zone underlying sediment of variable conductance (m^2/d). Note that decreasing conductance significantly decreases the size of the peak in seepage produced by the fracture zone.

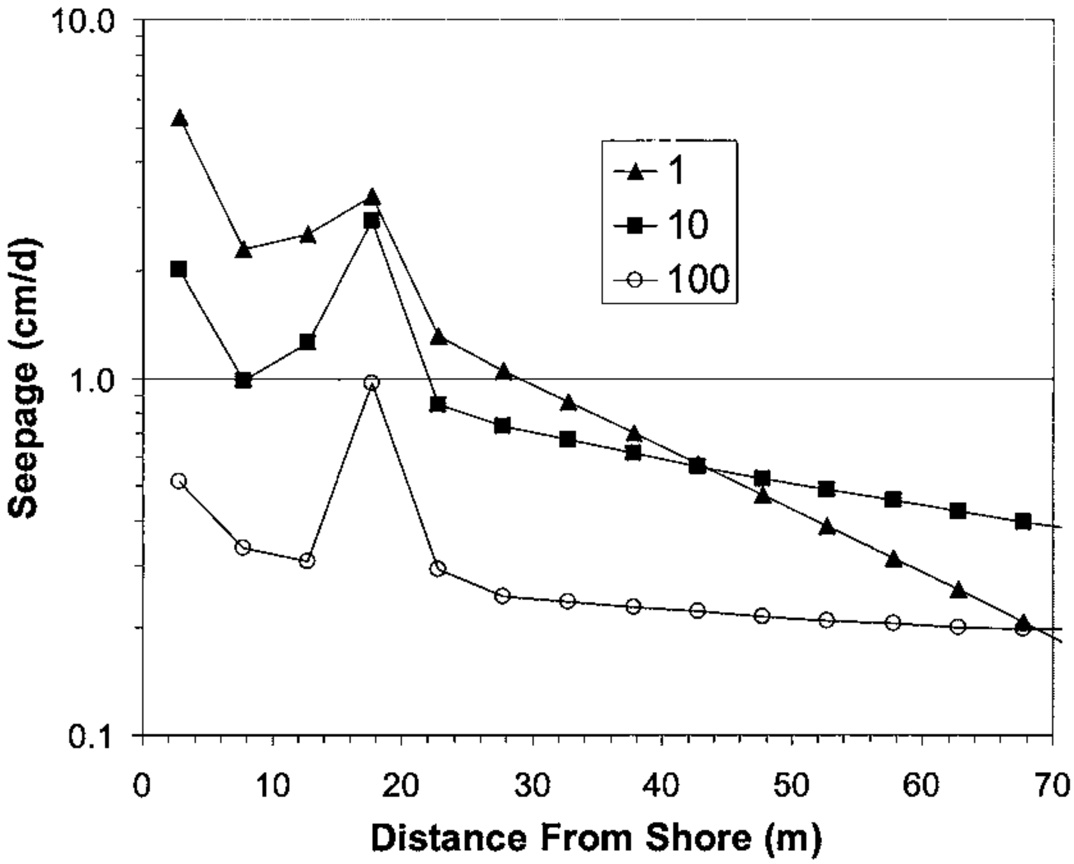

Figure 3-24: Semi-log plot of seepage vs. distance from shore of a high-K fracture zone combined with variable anisotropy (K_x/K_y). Note that unlike the behavior of a break in slope combined with anisotropy, no significant change in the size of the peak produced by the high-K fracture zone is seen.

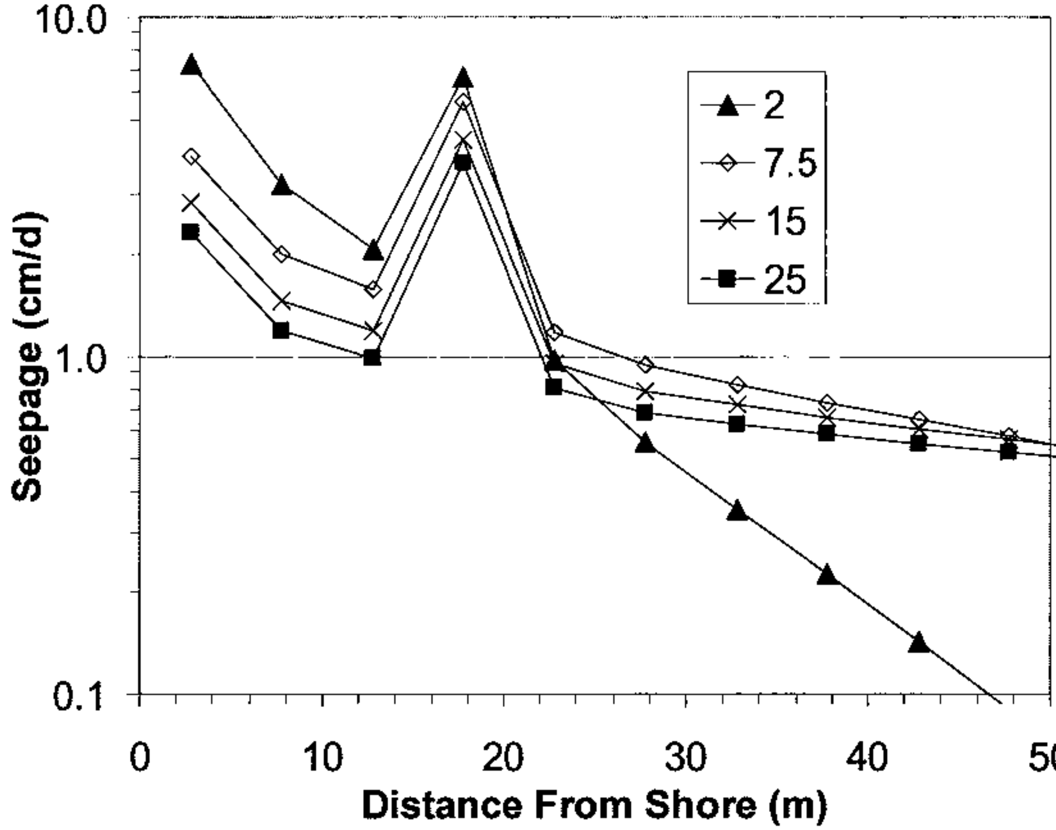

Figure 3-25: Semi-log plot of seepage vs. distance from shore of a high-K fracture zone combined with variable aquifer thickness (b_a/d). Note that like the behavior of a break in slope combined with various aquifer thickness, no significant change in the size of the peak produced by the high-K fracture zone is seen.

CHAPTER 4
DISCUSSION AND CONCLUSION

The parameter results from Chapter 3 are categorized in this chapter based on their influence on the distribution of seepage in lakes according to four distinct types of response:

1) Factors influencing overall seepage along a lake (Section 4.1)

2) Factors influencing the exponential distribution of seepage along a lake (Section 4.2)

3) Factors producing non-exponential seepage patterns (Section 4.3)

4) Factors of limited or no influence on seepage patterns (Section 4.4)

After this discussion is a summary of the implications of these results for field studies.

4.1 Factors Influencing Overall Seepage Along a Lake

Varying recharge uniformly between values of 1/24 to 2/3 of precipitation and varying the ratio of basin length (L) to lake radius (r) between values 2 to 7 distributed seepage rates uniformly along the lake model, and thus, had little influence on the exponential or non-exponential distribution of seepage. Because the lake-groundwater system was simulated using a symmetrical basin in which all recharge is diverted to an inflow lake, a change in recharge will be reflected proportionally in the overall volume of seepage received by the lake. Varying basin size increased the area over which the applied recharge rate occurred over, thus increasing overall flow diverted to the lake. Because this study only varied recharge rates uniformly across a basin, careful judgment must be taken in applying the results to all groundwater-lake systems. Non-uniform recharges rates due to uneven topography or different infiltration rates can result in the formation of a water table mound, especially in the case of flow-through lakes (e.g. Winter, 1976; Cherkauer and Zager, 1989). Such a situation may produce separate flow systems within the groundwater-lake system, which can produce a hinge line in the lake at which seepage reverses direction. Thus, the recharge model results are only applicable to local flow-systems in which the volume of basin recharge is discharging completely into a single lake basin. Under these conditions, the modeling showed that changing the recharge rates within a local basin in steady-state conditions had no effect on the distribution of seepage.

Careful attention must also be used when applying the modeling results to a 3-D system. Genereux and Bandopadhyay (2001) noted that in modeling a 2-D lake vs. a 3-D lake of the same basin size/lake radius and the same recharge rate applied uniformly across the top of each model that the 3-D model experienced seepage rates nearly three times higher than the 2-D lake. Such a difference is likely due to the larger percentage of basin area for recharge to occur over vs. lake area for discharge to be diverted to in a 3-D model. Thus, the actual values of seepage reported in this study are likely to be lower than values in a 3-D or field setting with identical model parameter values.

4.2 Factors Influencing the Exponential Distribution of Seepage

The following parameters and range of values modeled were found to influence the exponential slope of seepage versus distance from shore:

1) The ratio of aquifer thickness (b_a) to maximum lake depth (d) between values of 1.5 to 50

2) The uniform conductance (m^2/d) of lake bed sediments between values of 1.0 to 1.0×10^{-5}

3) Anisotropy (K_x/K_y) values between 1 to 500

The exponential distribution of seepage from shore is non-unique, since any combination of these three parameters may lead to a particular value of β measured along a lake seepage transect. When plotted as a function of β, the three parameters changed according to power functions with variable exponential slopes.

4.2.1 Aquifer Thickness

As a function of aquifer thickness, β decreased in absolute value by an exponential slope of -0.8 (Figure 4-1), and varied by a total factor of 14 using the range of modeled values of b_a/d. As a general rule, increasing b_a/d by a factor of 2 decreased β by a factor of 2. When $b_a/d < 10$ (or when then aquifer is less than 10x as thick as the maximum lake depth), seepage is concentrated closer to shore ($\beta > -0.02$), but is distributed more evenly along a lakebed when $b_a/d > 10$.

4.2.2 Uniform Sediment Conductance

As a function of sediment conductance, β decreased by an overall exponential slope of -0.5 (Figure 4-2), but the variation was not linear ($R^2 = 0.86$). For example, decreasing conductance by a factor of 100 decreased β by a factor of 2, decreasing conductance by a factor of 10,000 decreased β by a factor of 50, and decreasing conductance by a factor of 100,000 decreased β by a factor of 448. Thus, the slope of exponential decline changed significantly when very low values (< 0.01 m^2/d) of C were modeled, but had little effect on changing the slope when high values (> 0.01 m^2/d) of C were modeled.

4.2.4 Gradual Change Offshore in Conductance

When a gradual change in conductance (from 0.5 m^2/d to 0.005 m^2/d) along a 100 m length of a lake was modeled, β was significantly higher than that obtained from modeling a uniform conductance of 0.05 m^2/d. Thus, a significant enough transition offshore in either b_s or K_s results in a higher concentration of seepage closer to shore. In addition, b_s is indirectly related to conductance while K_s is directly related to conductance (see Equation 4), and thus, a linear increase in b_s results in an exponential decrease in conductance (Figure 4-3). Therefore, since conductance changes rapidly along a small length, modeling a linear increase in b_s results in a slight increase in seepage near shore that deviates from exponential seepage patterns.

4.2.3 Anisotropy

As anisotropy increased, β decreased by an exponential slope of -0.2 (Figure 4-4), which is minimal compared with exponential slopes produced by aquifer thickness and conductance variations. Decreasing K_x/K_y by a factor of 10 decreased β by a factor of 2, however, decreasing K_x/K_y by a factor of 100 decreased β by a factor of 4.3. However, β is approximately -0.02 when a K_x/K_y value of only 10 was modeled. Values of K_x/K_y above 20 produced a less significant change in β, and thus, are not as important in distributing seepage further from shore than values below 20.

4.3 Factors Producing Non-Exponential Seepage Patterns

The following factors and range of values resulted in the formation of non-exponential offshore peaks in seepage:

1) A localized thinning in lake bed sediment modeled at pinch-out percentages of 50%, 75%, 95%, 99.5%, and 100% (100, 50, 10, 1, and 0 cm of sediment).

2) A fracture zone 100x more conductive than the surrounding porous medium that was varied in length, connectivity to the lake, and orientation

3) A break in slope modeled at $\Phi = 11.3°$, $18.4°$, and $26.6°$

4.3.1 Localized Lake Sediment Heterogeneity

In the case of localized thinning of lake sediment, the magnitude of change (M) increased as the modeled percentage of pinch-out was increased. The greatest value of M, 150, was observed with a 100% pinch-out, and the lowest value of M, 2, was observed with a 50% pinch-out (Figure 4-5). Note that for cases in which the pinch-out is greater than 75%, M increases in value dramatically, but for values less than 75%, the change is less significant.

4.3.2 Fracture Zone

Increasing fracture zone length increased the value of M up to 7.1 when using a fracture zone of a length of 24.5 m and down to 2.6 when using a fracture zone length of 4 m (Figure 4-6). Thus, the size of a localized heterogeneity influences the size of the resulting peak in seepage. Increasing the distance of the fracture zone below the lake decreased M (M = 1.5 at 4 m away), and likewise, M increased in magnitude when in closer proximity to the lake (M = 7.1 when fully connected to lake, $F_c = 0$ m) (Figure 4-7). Orienting the fracture zone at angles closer to perpendicular to the lake (90°, 116.6°, 135°) produced greater values of M than those that were more parallel to the lake (45°, 153.4°, 180°), and thus, M plotted against ψ between values of 45° to 180° is parabolic (Figure 4-8). Reducing the conductance of lake sediment above a fracture zone significantly reduced the size of the peak produced by this fracture zone (Figure 4-9). A two order of magnitude contrast in conductance between lake sediment and the surrounding aquifer reduced this peak by nearly a factor of five. Thus, even a small amount of low-K lake sediment can buffer the effect of underlying heterogeneities on seepage patterns.

4.3.3 Lake Morphology (Break in Slope)

Increasing the vertex angle (Φ) at a break in lake slope resulted in only a slight increase in M at the location of the break in slope (Figure 4-10). This anomaly in seepage created by morphology drops off gradually towards the shore and drops off after the vertex point sharply (Figure 3-17). Thus, a break in lake slope by itself can create an increase in seepage, but it is smaller in magnitude than those caused by geologic heterogeneities and covers a broader region along the lake bed.

Increasing K_x/K_y was a significant factor in magnifying the peak in seepage produced by a break in lake slope (Figure 4-11). Decreasing conductance also significantly decreased the peak in seepage produced by a break in lake slope (Figure 3-19). In addition, a break in slope due to a localized thinning (pinch-out) of lake sediment also increased the peak in seepage at this location (Figure 3-21). However, the peak in seepage created by a break in slope alone was minimal compared with the addition of the sediment pinch-out.

4.4 Factors of limited or No influence on seepage patterns

Uniformly changing lake slope (θ) appeared to have no effect on changing seepage patterns. No changes in overall seepage volume, the slope of exponential decline of seepage from shore, or non-exponential peaks in seepage resulted from variations in this parameter (Figure 3-16). However, as noted in Section 4.3, a break in slope created a slight peak in seepage at the location of the break. A lake is likely to have a break in slope or transition offshore to a gentler slope of erosional or depositional origin, and thus, seepage rates observed along a single, constant slope are likely to be influenced by the diversion of groundwater from such breaks offshore. In addition, the maximum lake depth was held constant in all slope variations because a lake penetrating deeper into an aquifer produces a lower value of b_a/d, and thus, will influence the slope of exponential decline. Pfannkuch and Winter (1984), who modeled variations in lake morphology by increasing θ without a break in slope, therefore altering the maximum depth of the lake for each lake slope variation, observed a change in the slope of exponential seepage as a function of lake slope. Although a steeper lake slope is more likely than a shallow slope to penetrate deeper into the aquifer system, the modeling results in this paper show that the ratio of aquifer thickness to lake depth, not slope variations, are a parameter responsible for controlling the slope of exponential seepage.

Placing a sediment pinch-out various distances from shore and placing a fracture zone of an identical size, connectivity to lake, K, and orientation at various distances from shore both produced little variation in the relative size of the peak produced by each parameter (Figure 3-7 and Figure 3-11). However, the magnitude of the seepage peak decreased exponentially from shore similar to the rate at which surrounding seepage values decreased from shore. In addition, the effect of anisotropy on the size of a peak in seepage produced by a fracture zone was minimal (Figure 3-24).

Aquifer thickness variations also had little effect on changing the size of a peak in seepage produced by either a high-K fracture zone (Figure 3-25) or a break in slope (Figure 3-20)

4.5 Conclusions and Applications to Field Studies

Recharge and basin variation model results presented here are only applicable to local flow-systems in which the volume of basin recharge is discharging completely into a single lake basin. Under these conditions, the modeling showed that changing recharge rates within a local basin in steady-state conditions had no effect on the distribution of seepage. However, the relative changes in seepage rates produced by recharge and basin size variations in this study can produce measurable transient effects. When performing seepage studies on a lake, changes in precipitation and other diurnal fluxes should be carefully noted and multiple measurements should be performed at a single location to account for such variations in seepage rates.

Variations beneath the lake in the thickness of the aquifer (or the amount of penetration of the lake into the aquifer system), the conductance of lake bed sediments, and anisotropy effect the contrast between near shore and offshore seepage. An understanding of these three parameters is important when conducting a lake seepage study to predict the slope of exponential decline of seepage with distance from shore. For example, seepage should be distributed more evenly relative to distance from shore along a transect if it is either above low-K lake bed sediments, if maximum lake depth is shallow compared with the aquifer thickness, or if geologic material below the transect exhibits anisotropy in which K_x is much greater than K_y. Likewise, seepage should be focused closer to shore along a transect (i.e., slope steeper) if low-K lake sediment is thin or absent in the region, the lake extends deep into the aquifer, or if geologic material below the lake is isotropic (or $K_y > K_x$). However, the exponential distribution of seepage from shore is non-unique, since no more than one combination of these three parameters may lead to a particular value of β measured along a lake seepage transect.

Parameters that change on a local scale are more likely to cause small-scale seepage deviations than those that change on a regional scale. Small-scale geologic heterogeneities such as fracture zones, high-K lenses within aquifer material, localized sediment thinning (pinch-out) as well as breaks in lake slope under anisotropic conditions can all divert seepage across localized areas of a lake bed, producing significant peaks in seepage. Thus, such factors are important to consider when performing a water budget in order to account for the spatial distribution of seepage. Because geologic heterogeneities have been shown through this study to be the most influential factor controlling seepage patterns, detailed maps of the geologic materials below and near the lake including geophysical surveys should be performed to target areas where seepage anomalies are likely. Heterogeneities closer to shore are more likely to contribute a significant amount of seepage to a water budget than those further from shore, especially if the exponential slope of seepage vs. distance from shore is high, as is the case with thin aquifers (low b_a/d), the presence of anisotropy, and laterally extensive low-K lake sediment. One important factor in determining the significance of the change in seepage is the contrast in hydraulic conductivity between lake bed sediments and the local aquifer. The conductance of lake bed sediment and anisotropy should be estimated to determine whether heterogeneities or breaks in lake slope will produce significant localized changes in seepage rates. However, most of the features identified create changes in seepage that can be observed only at small scales, so water budget calculations will continue to depend on detailed field observations.

Research from both modeling and field measurements has shown that lakes are commonly characterized by an exponential decrease in seepage with increasing distance offshore. However, field data has also revealed deviations from this decay pattern. This study used groundwater modeling to examine the factors that create deviations from uniform exponential decline in seepage from shore produced by geologic heterogeneities and lake morphology. In particular, the modeling examined in more detail than previous studies how peaks in seepage are created. The modeling assessed the sensitivity of factors known to be influential and investigated new factors. This modeling can help guide field studies by providing geologic examples of what creates deviations from exponential decline in seepage away from a lake shore.

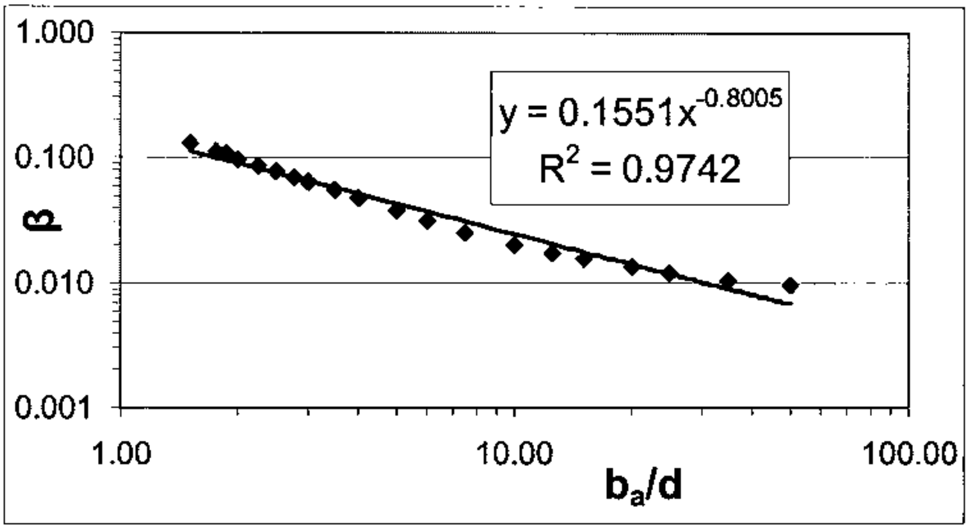

Figure 4-1: β as a function of aquifer thickness (b_a/d) variations. Note that this function decreased by exponential slope of -0.8, and increasing b_a/d by a factor of 2 decreased β by a factor of 2.

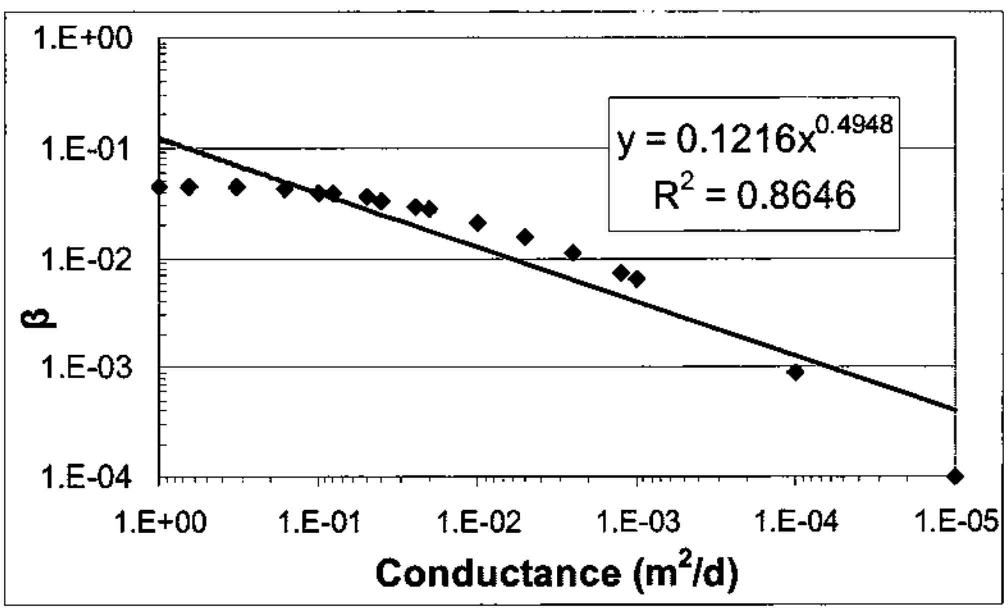

Figure 4-2: β as a function of sediment conductance (m^2/d) variations. This function decreased by an overall exponential slope of -0.5, but the variation was not linear ($R^2 = 0.86$). For example, decreasing conductance by a factor of 100 decreased β by a factor of 2 while decreasing conductance by a factor of 100,000 decreased β by a factor of 448.

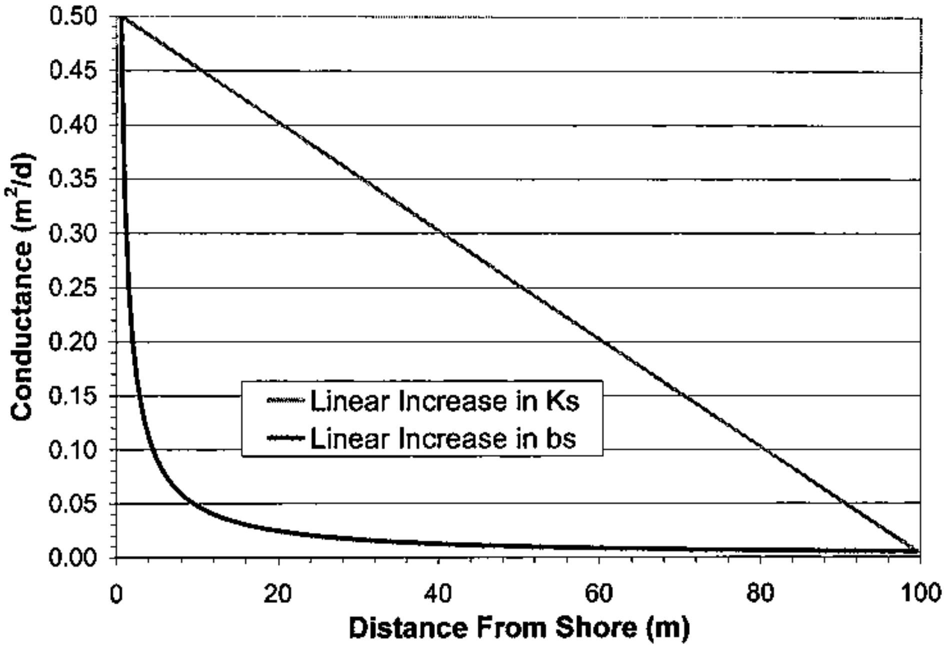

Figure 4-3: Plot of conductance vs. distance from shore for a linear increase in b_s and a linear decrease in K_s. Note that b_s is indirectly related to conductance while K_s is directly related to conductance (see Equation 4), and thus, a linear increase in b_s results in an exponential decrease in conductance.

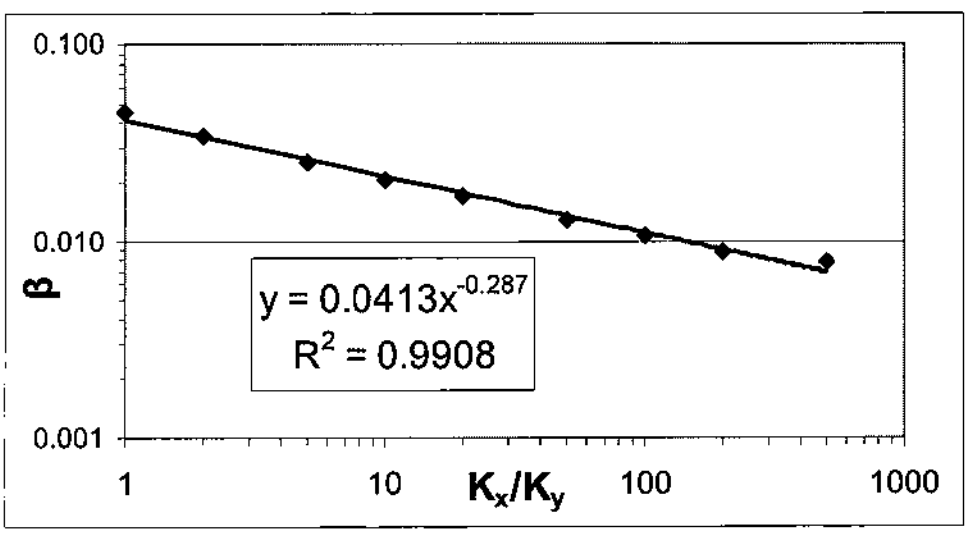

Figure 4-4: β as a function of anisotropy (K_x/K_y) variations. This function decreased by an exponential slope of -0.287, which is minimal compared with exponential slopes produced by aquifer thickness and conductance variations. Decreasing K_x/K_y by a factor of 10 decreased β by a factor of 2, however, decreasing K_x/K_y by a factor of 100 decreased β by a factor of 4.3.

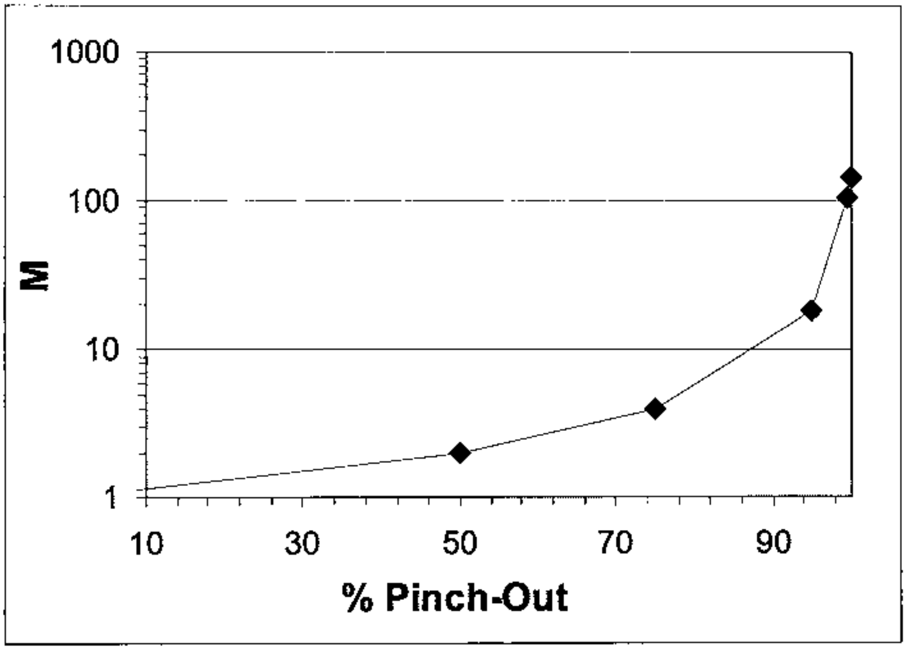

Figure 4-5: M vs. % pinch-out of lake sediment. The greatest value of M, 150, was observed with a 100% pinch-out, and the lowest value of M, 2, was observed with a 50% pinch-out.

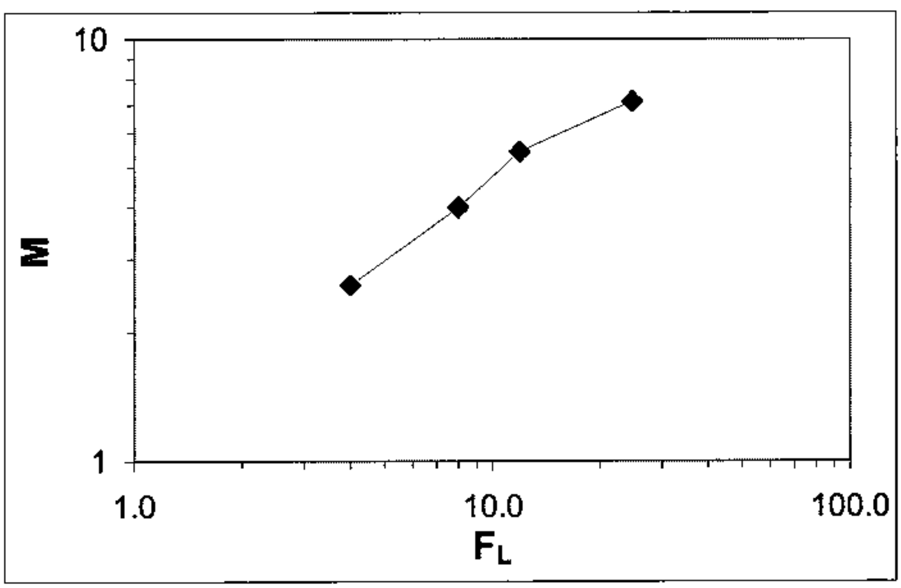

Figure 4-6: M vs. fracture zone length (m). A fracture zone of a length of 24.5 m produced a peak of M = 7.1, which reduced down to down to M = 2.6 when using a fracture zone length of 4 m.

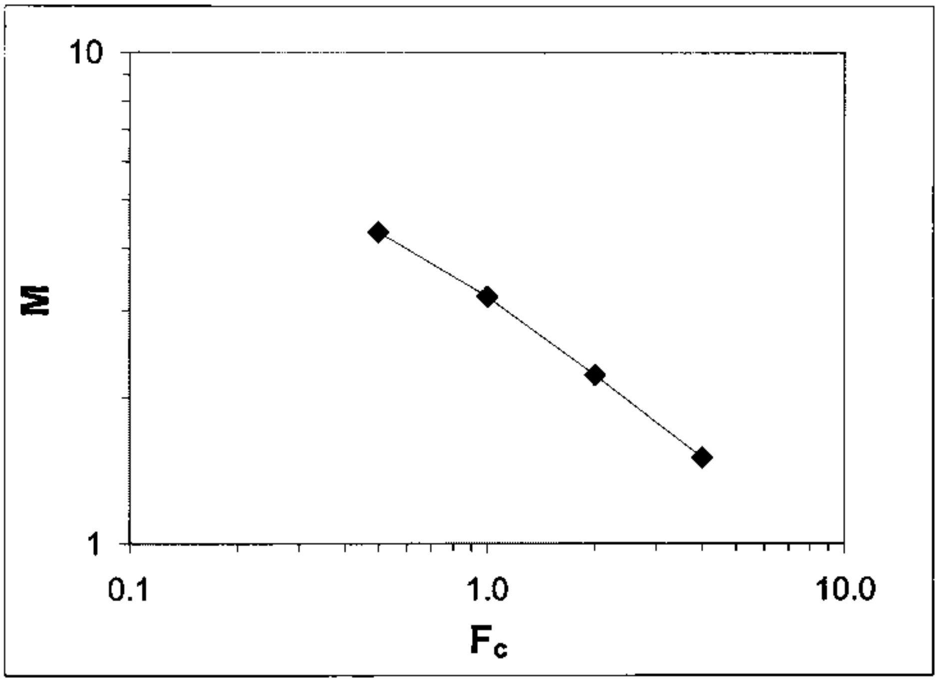

Figure 4-7: M vs. fracture zone connectivity (m). Decreasing the proximity of the fracture zone to the lake decreased M (M=1.5 at 4 m away), and likewise, M increased in magnitude when in closer proximity to the lake (M = 7.1 when fully connected to the lake, $F_c = 0$ m).

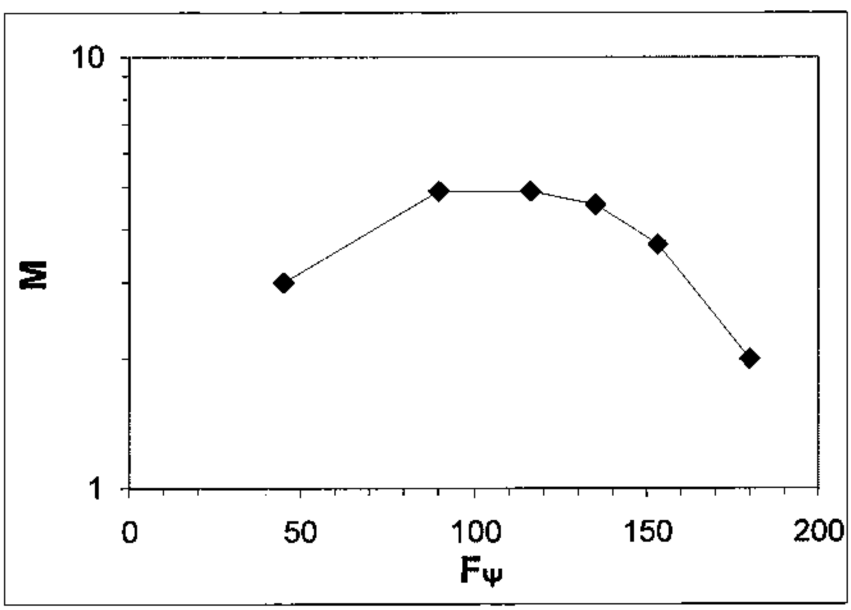

Figure 4-8: M vs. fracture zone orientation (degrees). Orienting the fracture zone at angles more perpendicular to the lake (90° and 135°) produced greater values of M than those that were oriented closer to parallel to the lake (0° and 45°).

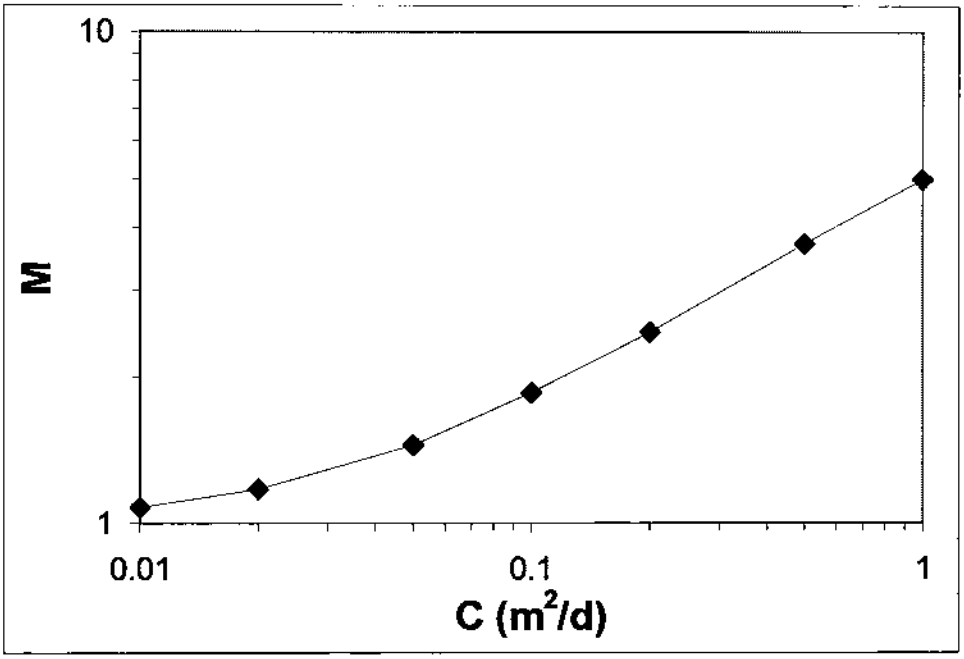

Figure 4-9: Various sediment conductance (m^2/d) with corresponding values of M produced by an identical fracture zone. Note that changing conductance by two orders of magnitude decreases the size of the peak produced by the fracture zone by a factor of five.

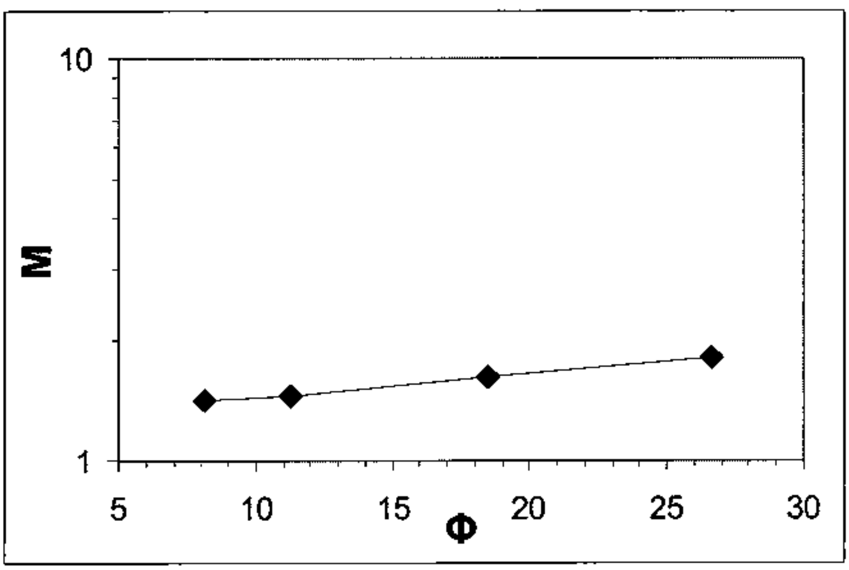

Figure 4-10: M vs. various break in slope vertex angles (degrees). Increasing the vertex angle resulted in an increased value of M at the location of the break in slope.

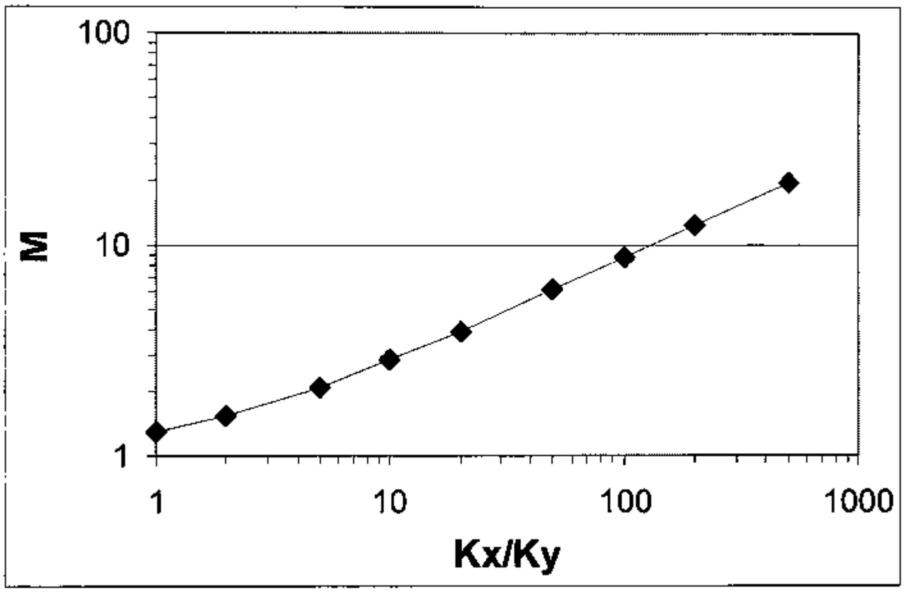

Figure 4-11: Various values of K_x/K_y with corresponding values of M produced by a 26.6° break in lake slope. Note that anisotropy has a significant effect in magnifying the size of the peak produced by such a morphology.

REFERENCES

Anderson, R.H., 1987. Geophysical determination and computer modeling of groundwater flux through lake sediments: Lake St. Clair, Michigan/Ontario. M.S. Thesis, University of Wisconsin-Milwaukee, WN, USA, 152 p.

Anderson, M.P. and Woessner, W.W., 1992. Applied groundwater modeling: simulation of flow and advective transport. San Diego, Academic Press, Inc., 381 p.

Asbury, C.E., 1990. The role of groundwater seepage in sediment chemistry and nutrient budgets in Mirror Lake, New Hampshire. PhD dissertation, Cornell University, Ithaca, NY, 275 p.

Connor, J.N. and T.V., Belanger, 1981. Groundwater seepage in Lake Washington and the Upper St. John's River Basin, Florida. *Water Resources Bulletin* 17, no. 5: 799-805.

Cherkauer, D.S. and McKereghan, P.F., 1991. Groundwater discharge to lakes: focusing in embayments. *Ground Water* 29, no. 1: 72-80.

Cherkauer, D.S. and Nader, D.C., 1989. Distribution of groundwater seepage to large surface-water bodies: the effect of hydraulic heterogeneities. *Journal of Hydrology* 109, no. 1-2: 151-165.

Cherkauer, D.S. and Zager, J.P., 1989. Groundwater interaction with a kettle-hole lake: relation of observations to digital simulations. *Journal of Hydrology* 109, 167-184.

Environmental Simulations, Inc, 2004. Groundwater Vistas Version 4 Manual. Reinholds, PA, 366 p.

Erikson, D.R., 1981. A study of littoral groundwater seepage at Williams Lake, Minnesota using seepage meters and wells. M.S. Thesis, University of Minnesota, Minneapolis, MN, USA, 135 p.

Federer, C.A., Flynn, L.D., Martin, C.W., Hornbeck, J.W., and Pierce, R.S., 1990. Thirty years of hydrometeorologic data at the Hubbard Brook Experimental Forest, New Hampshire. General Technical Report NE-141. Radnor, Pennsylvania: U.S. Department of Agriculture Forest Service, Northeastern Forest Experiment Station.

Freeze, R.A. and Cherry, J.A., 1979. Groundwater. Prentice-Hall, Englewood Cliffs, New Jersey, USA, 604 pp.

Genereux, I. and Bandopadhyay, T., 2001. Numerical investigations of lake bed seepage patterns: effects of porous medium and lake properties. *Journal of Hydrology* 241, 286-303.

Guyonnet, D.A., 1991. Numerical modeling of effects of small-scale sedimentary variations on groundwater discharge into lakes. *Limnology and Oceanography* 36, no. 4: 787-796.

Heaney, M., 2007. Marine Resistivity as a tool for characterizing zones of seepage at Lake Lacawac, PA. M.S. Thesis, Department of Geology, Temple University, Philadelphia, PA, 108 p.

Hunt, R.J., Haitjema, H.M., Krohelski, J.T., and Feinstein, D.T., 2003. Simulating ground water-lake interactions: approaches and insights. *Ground Water* 41, no. 2: 227-237.

John, P.H. and Lock, M.A., 1977. The spatial distribution of groundwater discharge into the littoral one of a New Zealand Lake. *Journal of Hydrology* 33, 391-395

Kalbus, E., Reinstorf, F., and Schirmer, M., 2006. Measuring methods for groundwater – surface water interactions: a review. *Hydrology and Earth System Sciences* 10: 873-887.

Kishel, H.F. and Gerla, P.J., 2002. Characteristics of preferential flow and groundwater discharge to Shingbee Lake, Minnesota, USA. *Hydrological Processes* 16: 1921-1934.

Krabbenhoft, D.P. and Anderson, M.P., 1986. Use of a numerical groundwater flow model for hypothesis testing. *Ground Water* 24: 49-50.

Lee, D.R., 1977. A device for measuring seepage flux in lakes and estuaries. *Limnology and Oceanography: Methods* 22, 140-147.

Lee, D.R., Cherry, J.A., and Pickens, J.F.,1980. Groundwater transport of a salt tracer through a sandy lakebed. *Limnology and Oceanography* 25, no. 1: 45-61.

McBride, M. and Pfannkuch, H., 1975. The distribution of seepage within lakebeds. *Jour. Research U.S. Geol. Survey* 3, 505-512.

McDonald, M.G. and Harbaugh, A.W., 1988. A modular three dimensional finite difference groundwater flow model. *USGS Survey Techniques of Water-Resources Investigations*, book 6, chap. A1, 586pp.

Mitchell, N., Nyquist, J.E., Toran, L.E., Rosenberry, D.O., and Mikochik, J.S., 2007. Electrical resistivity as a tool for identifying geologic heterogeneities which control seepage at Mirror Lake, NH. Proceedings of the Annual Symposium on the Application of Geophysics to Engineering and Environmental Problems, Philadelphia, PA, April 6-10, 2008, 11 p.

Munter, J.A. and Anderson, M.P., 1981. The use of groundwater flow models for estimating lake seepage rates. *Ground Water* 19, no. 6: 608-612.

Pfannkuch, H.O. and Winter, T.C., 1984. Effect of anisotropy and groundwater system geometry on seepage through lakebeds, 1. Analog and dimensional analysis. *Journal of Hydrology* 75, 213-237.

Sebestyen, S.D. and Schneider, R.L., 2001. Dynamic temporal patterns of nearshore seepage flux in a headwater Adirondack Lake. *Journal of Hydrology* 247, 137-150.

Schneider, R.L., Negley, T.L., and Wafer, C., 2005. Factors influencing groundwater seepage in a large, mesotrophic lake in New York. *Journal of Hydrology* 310, 1-16.

Rosenberry, D.O., 2000. Unsaturated-zone wedge beneath a large, natural lake. *Water Resources Research* 36, no.12: 3401-3409.

Rosenberry, D.O., 2005. Integrating seepage heterogeneity with the use of ganged seepage meters. *Limnology and Oceanography: Methods* 3, 131-142.

Shaw, R.D. and Prepas, E.E., 1990a. Groundwater-lake interactions: I. Accuracy of seepage meter estimates of lake seepage. *Journal of Hydrology* 119, 105-120.

Shaw, R.D. and Prepas, E.E., 1990b. Groundwater-lake interactions: II. Nearshore seepage patterns and the contribution of groundwater to lakes in Central Alberta, *Journal of Hydrology* 119: 121-136.

Taylor, R.W. and Cherkauer, D.S., 1984. The application of combined seismic and electrical measurements to the determination of the hydraulic conductivity of a lake bed. *Ground Water Monitoring Review* 4, no. 4: 78-85.

Tiedeman, C.R., Goode, D.J., and Hsieh, P.A., 1998. Characterizing a ground water basin in a New England mountain and valley terrain. *Ground Water* 36, no. 4: 611-620.

Winter, T.C., 1976. Numerical simulation analysis of the interaction of lakes and groundwater. *USGS Professional Paper* 1001, 1-45.

Winter, T.C., 1981. Effects of water table configuration on seepage through lakebeds. *Limnology and Oceanography* 26, no. 5: 925-934.

Winter, T.C., 1984. Geohydrologic setting of Mirror Lake, West Thornton, New Hampshire. *USGS Water Resources Investigations Report* 84-4266.

Woessner, W.W. and Sullivan, K.E., 1984. Results of seepage meter and mini-piezometer study, Lake Mead, Nevada. *Ground Water* 22, no. 5: 561-568.